3

Modular Walking Robots

Ion Ion, Ion Simionescu, Adrian Curaj and Alexandru Marin
Politehnica University of Bucharest
Romania

1. Introduction

Since ancient times, Man has been tempted to imagine, conceive and accomplish machines, which can imitate patterns of the Nature. It was even born the belief that people building mechanical patterns, similar to those of other beings, had a better chance, to discover the secrets of life. The way animals walk, the way birds fly, have always been and it will probably remain the sources of inspiration and tasks of the scientific research.

The animals using their feet for walk can move freely, with substantive easiness in comparison with what the man-made robot can do. Animals' locomotion is superior to that of the wheeled or caterpillared robot, both energetically and operationally speaking, as well as from the point of view of its stability, irrespective of the terrain the movement happens on. As compared to the Nature's achievements, the Man, God's pride, thanks to his cleverness and skills, succeeded to grasp many secrets of his creator, but he is still far from the Latter's accomplishments. Never disheartened with failures Man has created instruments for permanent investigation and success has not failed to arrive.

No matter what the previous generations imagined or not, the present one is creating things, that provide solutions to many of his strives and dreams, and this thank to the stored knowledge and the fresh opportunities of the technology which is in its full swing.

Studying the simplest but the most important movement types, such as the man's and the animals' movement, has been the scientists' most ancient preoccupation since the beginning of time. Mankind is so attached to the anthropomorphism, as it is almost impossible for it to conceive or imagine automatic systems, even equipped with artificial brain, which are not anthropomorphic.

In order to reach areas hard to get to, and where Man's life were jeopardized, the scientific research in time, and for different purposes, achieved mechanisms that thanks to their skills could cover several fields. Due to the special circumstances, regarding the vegetation and the terrain's state, and viewing the environment protection, the wheeled or the caterpillar machines, aiming at such applications, have a restrained mobility and thus, they considerably destroy the environment, the vegetation, bushes and the young trees, when passing through.

Walking robots protect the environment in a much better way, as their contact to the terrain is discrete, which considerably diminishes the area underwent to crushing; the robot's weight can be optimally distributed all over its leaning surface, by controlling the forces.

Source: Climbing & Walking Robots, Towards New Applications, Book edited by Houxiang Zhang,
ISBN 978-3-902613-16-5, pp.546, October 2007, Itech Education and Publishing, Vienna, Austria

Altering the distance to the ground, the robot can pass over young trees or other vegetation, growing in the passage area.

Avoiding hurdles such as logs or tree trunks is a considerable advantage. Likewise, the movement on an unarranged terrain represents another advantage of the walking robot, as compared to the other types of vehicles.

Unlike the wheeled or caterpillar robot, the walking robot is a mechatronic system, its practical use requiring both the computer-assisted surveillance and the thorough checking by the movement systems. In this century, the locomotion using feet as a movement system was reckoned an inefficient movement means. Nevertheless, if it is take into consideration the infrastructure's costs to artificially create the roads for the wheeled robot or own roads for the caterpillar robot, arguments for these two robot types diminish in some of the cases.

Walking main feature is the very fact that the movement is not affected by the terrain's configuration. More and more applications requiring movement on a natural, unarranged terrain, made the feet-movement solution become more and more attractive.

Here there are the main features justifying the superiority of the walking robot as compared to the wheeled or caterpillared ones (Hiller M., Muller J., Roll U., Schneider M., Scroter D., Torlo M. & Ward D., 1999):

- the capability to move on unarranged terrains;
- the walking robot can step over certain hurdles by changing its height (terrain clearance);
- the possibility to change the configuration of the walking robot's shift system;
- the feet's contact to the terrain is discontinuous (it is accomplished only in the leaning phase), when a foot has the opportunity to select the contact point, while descending on the terrain, contingent of the latter's surface;
- the possibility to move on a soft terrain, which is sometimes more difficult for the wheeled or the caterpillar robot;
- the walking robot's active suspension accomplished by setting the proximity and force sensors in the outermost part of feet, enables the movement on uneven terrain under stable circumstances;
- the specific energy consumption is smaller with the movement on natural unarranged terrains as against other types of mobile robots;
- the better preservation of the terrain, that the robot moves on, especially in case it is made use of in specific farming or forestry activities.

Its apparent density grows higher than the normal values by the terrain settlement, namely its total porosity goes lower than the usual values. The artificial or anthrop sinking happens as a result of the heavy, insensible traffic, during the farming season, because of the transportation or for other reasons. The terrain settlement (compactness) is a process specific to the modern, intensive and strongly mechanized farming and the higher the mechanization level, the deeper the sinking.

The terrain compactness has many negative effects, whatever its nature. Thus, it diminishes the terrain's capability to keep water, it reduces the aeration and often considerably decreases the endurance to penetration and makes the terrain hard to plough. As a result of the terrain's decaying its productivity strongly drops and the crops sometimes diminish by 50 percents as compared to that on non-compacted terrains. Among the drawbacks of the walking robot, here they are some worth to remind:

- the movement checking is rather sophisticated thank to the large number of freedom degrees;
- they develop rather low speed;
- the energy consumption is higher than with the wheeled robot or that on caterpillars because of the many accelerations and decelerations of some elements in the mechanical system, during walking;
- they claim bigger manufacture, maintenance and the exploitation costs.

2. Structure of Walking Robot Displacement Systems

Some of the most significant components of the walking robots are the mechanisms of the displacement systems. The mechanisms of the displacement system can have three or more degrees of freedom, and are built so that the lower end of the last element, termed *P*, to follow any trajectory from the task space. Therefore, the point *P* must gets over an adequate trajectory with respect to the robot platform. This trajectory is corresponding to the gait type for the displacement. Some of these mechanisms have a simple structure and one or two degrees of freedom, so that the shape of the trajectory of the point *P* may be very little adjusted. These displacement systems may be commanded and controlled using the simple equipments. The utilization of the mechanisms with complicated structure, with many ways of adjustment, capable to ensure the displacements of the walking robot in the various conditions, involves existence of a very elaborate control equipment.

Generally, the mechanisms for the displacement systems may be divided into two categories:

- plane linkages, with the frame can rotates around a vertical axis fixed on the platform of the walking machine;
- spatial linkages.

The plane linkages have commonly two degree of freedoms and can be very simple, consisting of two links, or with a very complicated structure.

At all this, the lower end of the last link of the leg can get over any spatial trajectory in the work space.

In Fig. 1 is shown the Bessonov (Bessonov A.P. & Umnov N.V., 1973) leg mechanism, with nine elements and eleven pairs. This is a triple closed mechanism with two degrees of freedom.

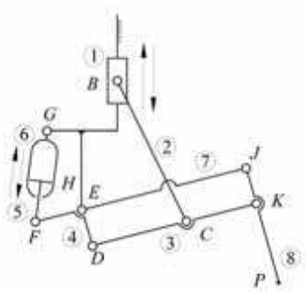

Fig. 1. Bessonov type leg mechanism

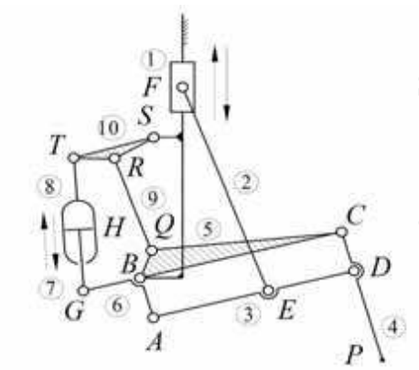

Fig. 2. *ODEX*-type leg mechanism

The *ODEX*-type leg mechanism (Song S.M. & Waldron K.J., 1989) is displayed in Fig. 2. This mechanism with four loops has eleven elements, 14 kinematics pairs and two degrees of freedom.

An orthogonal legged walking robot (Bares J) is shown in Fig. 3. The robot has al least two movement devices and each leg can exhibit an overlapping gait with respect to the other ones. Each leg is made of three links, serially connected through three driven pairs.

In Fig. 4 is shown a walking robot with six legs (Garrec P.). Each leg consist of a plane mechanism with one degree of freedom and constituted in such a way that the circular movement of a member driven by a motor is expressed by a horizontal rectilinear movement of the lower end of the last link. Each leg is connected to the platform by a revolute pair with vertical axis.

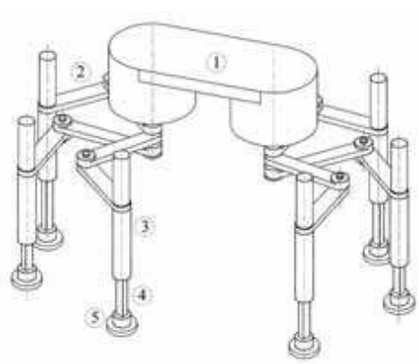

Fig. 3. A model of walking robot with six legs

The MERO experimental modular walking robot, built and tested at POLITEHNICA University of Bucharest, is shown in Fig. 5.

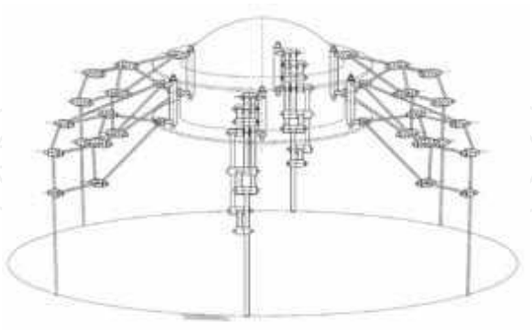

Fig. 4. Walking robot with six legs (Garrec P)

Fig. 5. MERO modular walking robot

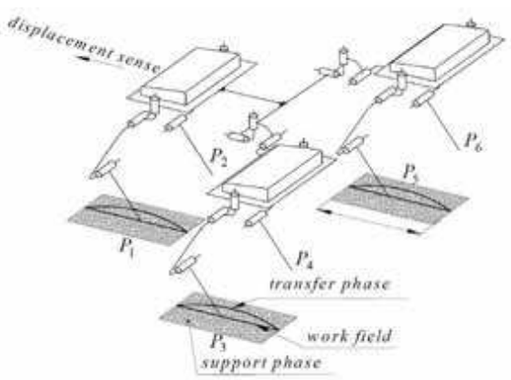

Fig. 6. Model of MERO walking modular robot

3. Kinematics Analysis of Displacement Systems

3.1. Mathematical model of gait for walking robots

The walking robot, unlike the wheels or caterpillars one, uses devices analogous to the man or animal legs. Unlike the wheel, the leg is not a system of continuous locomotion. Therefore, it has to be lifted away from the support phase, moved towards the advance direction of the walking robot and then laid down, following another cycle of another leg. As the walking robot has two or more legs, these moves have to be coordinated so that the move is ensured in conditions of the stability of the system. In order to allow a theoretical approach of the gait of the walking robot it is necessary to define a lot of terms. To achieve and manage a walking robot it is necessary to know all the walking possibilities, because the selection of the legs number and its structure depends on the selected type of the gait. The selection of the type of gait is a very complicated matter, especially in the real conditions of walking on the rough terrain. Therefore, it is necessary that the terrain surface to be selected before the type of gait is chose. According to the definitions given by McGhee (McGhee R.B. & Frank A.A., 1968), (McGhee R.B. & Orin D.E., 1976) and his collaborators, completed by Song and Waldorn (Song S.M. & Waldron K.J., 1989), the gait can be periodic or non-periodic. According to these definitions it can state the following.

The transfer phase of a leg is the period of time when the foot is not in contact with the terrain; the period of time in which this phase occurs is marked by τ. The leg state of a leg in the transfer phase is 1.

The support phase of a leg is the period of time in which the foot is in contact with the terrain; the period of time when this phase occurs is called by ς. The leg state of a leg in the support phase is 0.

The gait is *periodic* if the similar states of the same leg, during successive strokes occur at the same time interval for all the legs; a different type of gait is the aperiodic gait; the period of time when a step of the periodic gait occurs is called *cycle time*.

The *duration of a cycle time T* is the duration of a complete cycle of locomotion of a leg, during a periodic gait and it results from the following equation: $T = \varsigma + \tau$.

3.2 Kinematics analysis of leg mechanisms

3.2.1 Positions of elements

The walking robots are able to move on a terrain with irregular surface. As a result, the leg mechanisms must have at least three degrees of freedom in the transfer phase [Ion I., Simionescu I. & Curaj A. 2003), (McGhee R.B., Frank A.A., 1968), (Song S.M. & Waldron K.J., 1989). An usually kinematics scheme for the leg mechanisms is displayed in Fig. 7.

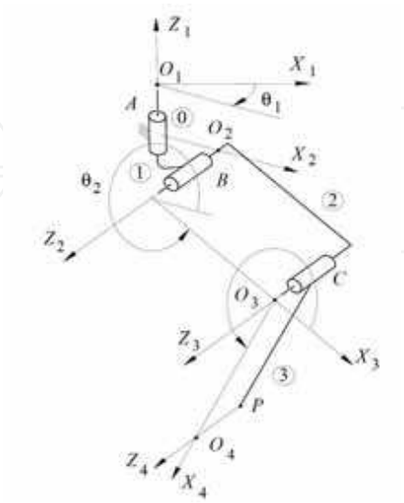

Fig. 7. Kinematics scheme of leg mechanism

This mechanism is build by three links, serially connected by three revolute pairs. All of the joints are driving ones. The lower end of the link (**3**) can be moved along an any spatial trajectory comprises in the operating field, with respect to the robot platform, with a pre-established displacement law.

The goal of the inverse kinematics analysis is to determine the variables of the driving pairs, i.e. the generalized coordinates, with respect to the position of the lower end of the link (**3**). The position of the point *P*, located to the lower end of the link (**3**), is defined with respect to the Denavit - Hartenberg axes system attached to this element [Denavit J., & Hartenberg R.S, 1955), (Uicker J.J.jr., Denavit J., Hartenberg R.S. 1965) by the coordinates x_{4P}, y_{4P} and z_{4P}. The position of the point *P* with respect to the Denavit - Hartenberg system $O_1x_1y_1z_1$ attached to the robot platform (**0**) may be calculated by equation:

$$\begin{Vmatrix} 1 \\ x_{1P} \\ y_{1P} \\ z_{1P} \end{Vmatrix} = \mathbf{A}_1\mathbf{A}_2\mathbf{A}_3 \begin{Vmatrix} 1 \\ x_{4P} \\ y_{4P} \\ z_{4P} \end{Vmatrix}. \tag{1}$$

The origin O_1 of the coordinate axes system attached to the robot platform is chosen in a convenient mode and specified by the distance s_1. The direction of the O_1x_1 axes is arbitrary and must be specified.

The leg mechanism shown in Fig. 7 has the following features:

- the axis of the pair *A* is perpendicular to the axis of the pair *B*;
- the axis of the pair *B* is parallel to the axis of the pair *C*.

Consequently, $\alpha_1 = \pi/2$, $\alpha_2 = \alpha_3 = 0$, $s_2 = s_3 = 0$, $a_1 = 0$.

The matrix equation (1) is equivalence to three scalar equations. In order to perform an inverse kinematics analysis of the leg mechanism, the system (1) is solved with respect to the unknowns θ_1, θ_2 and θ_3. This is a nonlinear system and must be used an adequate numerical method, for example the Newton – Raphson method (Simionescu I., Dranga M. & Moise V. 1995), (Hildegrand F.B. 1956). If the pair i is prismatic one, the angle θ_i is known exactly, and the distance s_i is unknown.

3.2.2 First time-derivatives of pair variables

Differentiating both sides of the equation (2) with respect to the time yields:

$$\begin{Vmatrix} 0 \\ \dot{x}_{1P} \\ \dot{y}_{1P} \\ \dot{z}_{1P} \end{Vmatrix} = \left(\frac{\partial \mathbf{A}_1}{\partial \theta_1} \mathbf{A}_2 \mathbf{A}_3 \frac{\mathrm{d}\theta_1}{\mathrm{d}t} + \mathbf{A}_1 \frac{\partial \mathbf{A}_2}{\partial \theta_2} \mathbf{A}_3 \frac{\mathrm{d}\theta_2}{\mathrm{d}t} + \right.$$

$$\left. + \mathbf{A}_1 \mathbf{A}_2 \frac{\partial \mathbf{A}_3}{\partial \theta_3} \frac{\mathrm{d}\theta_3}{\mathrm{d}t} \right) \begin{Vmatrix} 1 \\ x_{4P} \\ y_{4P} \\ z_{4P} \end{Vmatrix}. \tag{2}$$

Noting that the problem is to be adapted to computer operation, a linear operator matrix $\mathbf{Q}_\theta$ is introduced to perform the indicated differentiation through the following definition

$$\frac{\partial \mathbf{A}_i}{\partial \theta_i} = \mathbf{Q}_\theta \mathbf{A}_i .$$

Under this definition, the $\mathbf{Q}_\theta$ is found to be (Uicker J.J.jr., Denavit J., Hartenberg R.S, 1965):

$$\mathbf{Q}_\theta = \begin{Vmatrix} 0 & 0 & 0 & 0 \\ 0 & 0 & -1 & 0 \\ 0 & 1 & 0 & 0 \\ 0 & 0 & 0 & 0 \end{Vmatrix}.$$

It provides a simplified method of taking the partial derivative, especially in computer operation. With these the equation (2) becomes

$$\begin{Vmatrix} 0 \\ \dot{x}_{1P} \\ \dot{y}_{1P} \\ \dot{z}_{1P} \end{Vmatrix} = \left(\mathbf{Q}_\theta \mathbf{A}_1 \mathbf{A}_2 \mathbf{A}_3 \frac{\mathrm{d}\theta_1}{\mathrm{d}t} + \mathbf{A}_1 \mathbf{Q}_\theta \mathbf{A}_2 \mathbf{A}_3 \frac{\mathrm{d}\theta_2}{\mathrm{d}t} + \right.$$
$$\left. + \mathbf{A}_1 \mathbf{A}_2 \mathbf{Q}_\theta \mathbf{A}_3 \frac{\mathrm{d}\theta_3}{\mathrm{d}t} \right) \begin{Vmatrix} 1 \\ x_{4P} \\ y_{4P} \\ z_{4P} \end{Vmatrix}. \quad (3)$$

Equating the matrices from equation (3) element for element, would produce a system of three linear equations in three unknowns, namely: $\frac{\mathrm{d}\theta_1}{\mathrm{d}t}$, $\frac{\mathrm{d}\theta_2}{\mathrm{d}t}$ and $\frac{\mathrm{d}\theta_3}{\mathrm{d}t}$.

3.3 Second time-derivatives of pair variables

Rather than to take the time-derivative of $\frac{\mathrm{d}\theta_i}{\mathrm{d}t}$, $i = \overline{1,3}$, from equations (3), it is convenient to continue to approach established above in differentiating the matrix equation (3). To facilitate the differentiation of this equation, it is first be necessary to find an expression for the time derivative of the matrix product

$$\mathbf{B}_i = \mathbf{A}_1 \ldots \mathbf{A}_{i-1} \mathbf{Q}_\theta \mathbf{A}_i \ldots \mathbf{A}_3,$$

that is

$$\frac{\mathrm{d}\mathbf{B}_i}{\mathrm{d}t} = \frac{\partial \mathbf{A}_1}{\partial \theta_1} \ldots \mathbf{A}_{i-1} \mathbf{Q}_\theta \mathbf{A}_i \ldots \mathbf{A}_3 \frac{\mathrm{d}\theta_i}{\mathrm{d}t} + \ldots + \mathbf{A}_1 \ldots \frac{\partial \mathbf{A}_{i-1}}{\partial \theta_{i-1}}$$
$$\mathbf{Q}_\theta \mathbf{A}_i \ldots \mathbf{A}_3 \frac{\mathrm{d}\theta_{i-1}}{\mathrm{d}t} + \mathbf{A}_1 \ldots \mathbf{A}_{i-1} \mathbf{Q}_\theta \frac{\partial \mathbf{A}_i}{\partial \theta_i} \ldots \mathbf{A}_3 \frac{\mathrm{d}\theta_i}{\mathrm{d}t} +$$
$$\ldots + \mathbf{A}_1 \ldots \mathbf{A}_{i-1} \mathbf{Q}_\theta \mathbf{A}_i \ldots \frac{\partial \mathbf{A}_3}{\partial \theta_3} \frac{\mathrm{d}\theta_3}{\mathrm{d}t}.$$

Again using the derivative operator to perform the differentiation, the time-derivative of the equation (3) is

$$\begin{Vmatrix} 0 \\ \ddot{x}_{1P} \\ \ddot{y}_{1P} \\ \ddot{z}_{1P} \end{Vmatrix} = \left(\mathbf{Q}_\theta \mathbf{Q}_\theta \mathbf{A}_1 \mathbf{A}_2 \mathbf{A}_3 \left(\frac{\mathrm{d}\theta_1}{\mathrm{d}t} \right)^2 + 2\mathbf{Q}_\theta \mathbf{A}_1 \mathbf{Q}_\theta \mathbf{A}_2 \mathbf{A}_3 \frac{\mathrm{d}\theta_1}{\mathrm{d}t} \frac{\mathrm{d}\theta_2}{\mathrm{d}t} + \right.$$
$$+ 2\mathbf{Q}_\theta \mathbf{A}_1 \mathbf{A}_2 \mathbf{Q}_\theta \mathbf{A}_3 \frac{\mathrm{d}\theta_1}{\mathrm{d}t} \frac{\mathrm{d}\theta_3}{\mathrm{d}t} + 2\mathbf{A}_1 \mathbf{Q}_\theta \mathbf{A}_2 \mathbf{Q}_\theta \mathbf{A}_3 \frac{\mathrm{d}\theta_2}{\mathrm{d}t} \frac{\mathrm{d}\theta_3}{\mathrm{d}t} + \quad (4)$$
$$+ \mathbf{A}_1 \mathbf{Q}_\theta \mathbf{Q}_\theta \mathbf{A}_2 \mathbf{A}_3 \left(\frac{\mathrm{d}\theta_2}{\mathrm{d}t} \right)^2 + \mathbf{A}_1 \mathbf{A}_2 \mathbf{Q}_\theta \mathbf{Q}_\theta \mathbf{A}_3 \left(\frac{\mathrm{d}\theta_3}{\mathrm{d}t} \right)^2 + \mathbf{Q}_\theta \mathbf{A}_1 \mathbf{A}_2$$
$$\left. \mathbf{A}_3 \frac{\mathrm{d}^2\theta_1}{\mathrm{d}t^2} + \mathbf{A}_1 \mathbf{Q}_\theta \mathbf{A}_2 \mathbf{A}_3 \frac{\mathrm{d}^2\theta_2}{\mathrm{d}t^2} + \mathbf{A}_1 \mathbf{A}_2 \mathbf{Q}_\theta \mathbf{A}_3 \frac{\mathrm{d}^2\theta_3}{\mathrm{d}t^2} \right) \begin{Vmatrix} 1 \\ x_{4P} \\ y_{4P} \\ z_{4P} \end{Vmatrix}.$$

Equating the matrices from equation (4) element for element, would produce a system of three linear equati-ons in three unknowns, namely $\frac{\mathrm{d}^2\theta_1}{\mathrm{d}t^2}$, $\frac{\mathrm{d}^2\theta_2}{\mathrm{d}t^2}$ and $\frac{\mathrm{d}^2\theta_3}{\mathrm{d}t^2}$. A new problem arises, however, when one of the pairs, for instance pair *i*, is prismatic. The $\mathbf{A}_i$ transformation matrix for this pair is essentially the same before. However, the angle θ_i is known exactly, and the distance s_i is unknown. The linear operator matrix $\mathbf{Q}_s$ is replaced by the operator $\mathbf{Q}_s$:

$$\frac{\partial \mathbf{A}_i}{\partial s_i} = \mathbf{Q}_s \mathbf{A}_i$$

Under this definition, the $\mathbf{Q}_s$ matrix is found to be [30]:

$$\mathbf{Q}_s = \begin{Vmatrix} 0 & 0 & 0 & 0 \\ 0 & 0 & 0 & 0 \\ 0 & 0 & 0 & 0 \\ 1 & 0 & 0 & 0 \end{Vmatrix}.$$

Fig. 8 displayed the kinematics scheme of the mechanical system of a walking robot achieved in modular structure. Each module is made by a platform which is joined with two legs. The modules are joined together by the connecting kinematics chains. These chains have three degrees of freedom and are made from two elements that are pinned together by three revolute pairs. Each first and last element of the connecting kinematics chain is joined to a module platform. All the joints of the connecting chain are driving ones. As a result, each kinematic chain is a sequence of three *R*-type active kinematics groups, connected in series (Simionescu I. & Moise V., 1999). It is considered a coordinate axes system attached to the platform of the first module. The axes of the Denavit – Hartenberg trihedrons (Denavit J. & Hartenberg R.S., 1955) are denoted with two indexes. The subscript index denotes the

number of the kinematics pair in the chain, and the superscript index denotes the number of the leg.

The coordinate of the support point P^i of the leg (i) with respect to the platform coordinate axes system $O_0X_0Y_0Z_0$ are:

$$\begin{Vmatrix} 1 \\ x_{0P}^i \\ y_{0P}^i \\ z_{0P}^i \end{Vmatrix} = \mathbf{A}_0^i \mathbf{A}_1^i \mathbf{A}_2^i \mathbf{A}_3^i \begin{Vmatrix} 1 \\ x_{4P}^i \\ y_{4P}^i \\ z_{4P}^i \end{Vmatrix}, \; i = 1, 2; \tag{5}$$

$$\begin{Vmatrix} 1 \\ x_{0P}^i \\ y_{0P}^i \\ z_{0P}^i \end{Vmatrix} = \mathbf{A}_0^i \mathbf{A}_1^7 \mathbf{A}_1^8 \mathbf{A}_1^9 \mathbf{A}_1^i \mathbf{A}_2^i \mathbf{A}_3^i \begin{Vmatrix} 1 \\ x_{4P}^i \\ y_{4P}^i \\ z_{4P}^i \end{Vmatrix}, \; i = 3, 4; \tag{6}$$

$$\begin{Vmatrix} 1 \\ x_{0P}^i \\ y_{0P}^i \\ z_{0P}^i \end{Vmatrix} = \mathbf{A}_0^i \mathbf{A}_1^{10} \mathbf{A}_1^{11} \mathbf{A}_1^{12} \mathbf{A}_1^i \mathbf{A}_2^i \mathbf{A}_3^i \begin{Vmatrix} 1 \\ x_{4P}^i \\ y_{4P}^i \\ z_{4P}^i \end{Vmatrix}, \; i = 5, 6. \tag{7}$$

In the direct kinematic analysis the variables of the all driving kinematic pairs are considered as known. The goal of the direct kinematics analysis is to simulate the displacement of the walking robot.

In the inverse kinematic analysis of the leg mechanism, the position x_{0P}, y_{0P}, z_{0P}, the velocity $\dot{x}_{0P}$, $\dot{y}_{0P}$, $\dot{z}_{0P}$ and the acceleration $\ddot{x}_{0P}$, $\ddot{y}_{0P}$, $\ddot{z}_{0P}$ of the point P with respect to the robot platform are considered as known. The unknowns of the problem are the variables of the driving pairs and their first and second time-derivative. The matrix equations (5), (6) and (7) are equivalent with three scalar equations and have six unknowns. As a result, three pair variables can be calculated by solving of the equations (5), (6) and (7) only. The remaining of three pair variables must by established so that the walking robot to adapt to the terrain in an optimum mode. The time-derivative of the variables of the driving pairs are calculated by solving the equation which arisen by differentiating of the equations (5), (6) and (7).l

$$\begin{Vmatrix} 1 \\ \dot{x}^i_{0P} \\ \dot{y}^i_{0P} \\ \dot{z}^i_{0P} \end{Vmatrix} = \left(\mathbf{A}^i_0 \mathbf{Q}_\theta \mathbf{A}^i_1 \mathbf{A}^i_2 \mathbf{A}^i_3 \frac{\mathrm{d}\theta_1}{\mathrm{d}t} + \mathbf{A}^i_0 \mathbf{A}^i_1 \mathbf{Q}_\theta \mathbf{A}^i_2 \mathbf{A}^i_3 \frac{\mathrm{d}\theta_2}{\mathrm{d}t} * \right.$$

$$\left. + \mathbf{A}^i_0 \mathbf{A}^i_1 \mathbf{A}^i_2 \mathbf{Q}_\theta \mathbf{A}^i_3 \frac{\mathrm{d}\theta_3}{\mathrm{d}t} \right) \begin{Vmatrix} 1 \\ x^i_{4P} \\ y^i_{4P} \\ z^i_{4P} \end{Vmatrix}, \; i = 1, 2;$$

$$\begin{Vmatrix} 1 \\ \dot{x}^i_{0P} \\ \dot{y}^i_{0P} \\ \dot{z}^i_{0P} \end{Vmatrix} = \left(\mathbf{A}^i_0 \mathbf{Q}_\theta \mathbf{A}^7_1 \mathbf{A}^8_2 \mathbf{A}^9_3 \mathbf{A}^i_1 \mathbf{A}^i_2 \mathbf{A}^i_3 \frac{\mathrm{d}\theta^7_1}{\mathrm{d}t} + \mathbf{A}^i_0 \mathbf{A}^7_1 \mathbf{Q}_\theta \mathbf{A}^8_2 \mathbf{A}^9_3 \mathbf{A}^i_1 \mathbf{A}^i_2 \mathbf{A}^i_3 \frac{\mathrm{d}\theta^8_2}{\mathrm{d}t} \right.$$

$$+ \mathbf{A}^i_0 \mathbf{A}^7_1 \mathbf{A}^8_2 \mathbf{Q}_\theta \mathbf{A}^9_3 \mathbf{A}^i_1 \mathbf{A}^i_2 \mathbf{A}^i_3 \frac{\mathrm{d}\theta^9_3}{\mathrm{d}t} + \mathbf{A}^i_0 \mathbf{A}^7_1 \mathbf{A}^8_2 \mathbf{A}^9_3 \mathbf{Q}_\theta \mathbf{A}^i_1 \mathbf{A}^i_2 \mathbf{A}^i_3 \frac{\mathrm{d}\theta^i_1}{\mathrm{d}t}$$

$$\left. + \mathbf{A}^i_0 \mathbf{A}^7_1 \mathbf{A}^8_2 \mathbf{A}^9_3 \mathbf{A}^i_1 \mathbf{Q}_\theta \mathbf{A}^i_2 \mathbf{A}^i_3 \frac{\mathrm{d}\theta^i_2}{\mathrm{d}t} + * \mathbf{A}^i_0 \mathbf{A}^7_1 \mathbf{A}^8_2 \mathbf{A}^9_3 \mathbf{A}^i_1 \mathbf{A}^i_2 \mathbf{Q}_\theta \mathbf{A}^i_3 \frac{\mathrm{d}\theta^i_3}{\mathrm{d}t} \right) \begin{Vmatrix} 1 \\ x^i_{4P} \\ y^i_{4P} \\ z^i_{4P} \end{Vmatrix},$$

$i = 3, 4;$

$$\begin{Vmatrix} 1 \\ \dot{x}^i_{0P} \\ \dot{y}^i_{0P} \\ \dot{z}^i_{0P} \end{Vmatrix} = \left(\mathbf{A}^i_0 \mathbf{Q}_\theta \mathbf{A}^{10}_1 \mathbf{A}^{11}_2 \mathbf{A}^{12}_3 \mathbf{A}^i_1 \mathbf{A}^i_2 \mathbf{A}^i_3 \frac{\mathrm{d}\theta^{10}_1}{\mathrm{d}t} + \mathbf{A}^i_0 \mathbf{A}^{10}_1 \mathbf{Q}_\theta \mathbf{A}^{11}_2 \mathbf{A}^{12}_3 \mathbf{A}^i_1 \mathbf{A}^i_2 \mathbf{A}^i_3 \frac{\mathrm{d}\theta^{11}_2}{\mathrm{d}t} + \right.$$

$$+ \mathbf{A}^i_0 \mathbf{A}^{10}_1 \mathbf{A}^{11}_2 \mathbf{Q}_\theta \mathbf{A}^{12}_3 \mathbf{A}^i_1 \mathbf{A}^i_2 \mathbf{A}^i_3 \frac{\mathrm{d}\theta^{12}_3}{\mathrm{d}t} + \mathbf{A}^i_0 \mathbf{A}^{10}_1 \mathbf{A}^{11}_2 \mathbf{A}^{12}_3 \mathbf{Q}_\theta \mathbf{A}^i_1 \mathbf{A}^i_2 \mathbf{A}^i_3 \frac{\mathrm{d}\theta^i_1}{\mathrm{d}t} +$$

$$\left. + \mathbf{A}^i_0 \mathbf{A}^{10}_1 \mathbf{A}^{11}_2 \mathbf{A}^{12}_3 \mathbf{A}^i_1 \mathbf{Q}_\theta \mathbf{A}^i_2 \mathbf{A}^i_3 \frac{\mathrm{d}\theta^i_2}{\mathrm{d}t} + + \mathbf{A}^i_0 \mathbf{A}^{10}_1 \mathbf{A}^{11}_2 \mathbf{A}^{12}_3 \mathbf{A}^i_1 \mathbf{A}^i_2 \mathbf{Q}_\theta \mathbf{A}^i_3 \frac{\mathrm{d}\theta^i_3}{\mathrm{d}t} \right) \begin{Vmatrix} 1 \\ x^i_{4P} \\ y^i_{4P} \\ z^i_{4P} \end{Vmatrix},$$

$i = 5, 6;$

4. Force Distribution in Displacement Systems of Walking Robots

The system builds by the terrain on which the displacement is done and the walking robot which has three legs in the support phase is statically determinate.

When it leans upon four (or more) feet, it turns in a statically indeterminate system.

The problem of determination of reaction force components is made in simplifying assumption, namely the stiffness of the walking robot mechanical structure and terrain.

For establishing the stable positions of a walking robot it is necessary to determine the forces distribution in the shifting mechanisms. In the case of a uniform and rectilinear movement of the walking robot on a plane and horizontal surface, the reaction forces do not have the tangential components, because the applied forces are the gravitational forces only.

Determination of the real forces distribution in the shifting mechanisms of a walking locomotion system which moves in rugged land at low speed is necessary for the analysis of stability. The position of a walking system depends on the following factors:

- the configuration of walking mechanisms;
- the masses of component elements and their positions of gravity centers;
- the values of friction coefficients between terrain and feet;
- the shape of terrain surface.
- the stiffness of terrain;

The active surface of the foot is relatively small and it is considered that the reaction force is applied in the gravity center of this surface. The reaction force represents the resultant of the elementary forces, uniformly distributed on the foot sole surface. The gravity center of the foot active surface is called *theoretical contact point.*

To calculate the components of reaction forces, namely:

- normal component $\overline{N}$, perpendicular on the surface of terrain in the theoretical contact point;
- tangential component $\overline{T}$, or coulombian frictional force, comprised in the tangent plane at terrain surface in the theoretical contact point,

it is necessary to determine the stable positions of walking robots (Ion I., Simionescu I. & Curaj A.,. 2002), (Ion I. & Stefanescu D.M., 1999).

The magnitude of $\overline{T}$ vector cannot be greater than the product of the magnitude of the normal component $\overline{N}$ by the frictional coefficient μ between foot sole and terrain. If this magnitude is greater than the friction force, then the foot slips down along the support surface to the stable position, where the magnitudes of this component decrease under the above-mentioned limit.

Therefore, the problem of determining the stable position of a walking robot upon some terrain has not a unique solution. For every foot is available a field which covers all contact points in which the condition $T \leq \mu N$ is true. The equal sign corresponds to the field's boundary.

The complex behavior of the earth cannot be described than by an idealization of its properties. The surface of terrain which the robot walks on is defined in respect to a fixed

coordinates system Oξηζ annexed to the terrain, by the parametrical equations ξ = ξ(*u*, *v*); η = η(*u*, *v*); ζ = ζ(*u*, *v*), implicit equation *F*(ξ,η,ζ) = 0, or explicit equation ζ = *f*(ξ,η).

These real, continuous and uniform functions with continuous first partial and ordinary derivative, establish a biunivocal correspondence between the points of support surface and the ordered pairs (*u*, *v*), where {*u*, *v*}∈ R. Not all partial first order derivatives are null, and not all Jacobians

$\frac{D(\xi,\eta)}{D(u,v)}; \frac{D(\eta,\zeta)}{D(u,v)}; \frac{D(\zeta,\xi)}{D(u,v)}$ are simultaneous null.

On the entire surface of the terrain, the equation expressions may be unique or may be multiple, having the limited domains of validity.

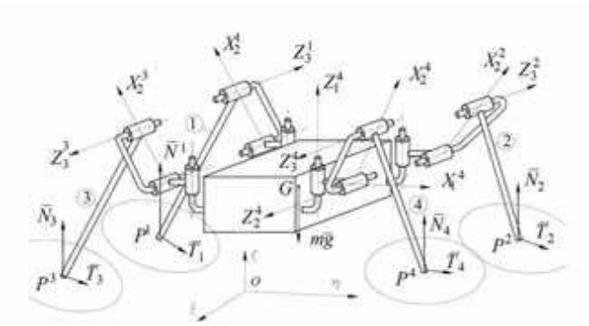

Fig. 8. The Hartenberg – Denavit coordinate systems and the reaction force components

The normal component $\overline{N}_i$ of reaction force at the P^i contact point of the leg *i* with the terrain is positioned by the direction cosine:

$$\cos\alpha^i = \frac{A_i}{\sqrt{A_i^2 + B_i^2 + C_i^2}}; \ \cos\beta^i = \frac{B_i}{\sqrt{A_i^2 + B_i^2 + C_i^2}};$$

$$\cos\gamma^i = \frac{C_i}{\sqrt{A_i^2 + B_i^2 + C_i^2}},$$

with respect to the fixed coordinate axes system, where:

$$A_i = \begin{vmatrix} \frac{\partial \eta^i}{\partial u_i} & \frac{\partial \zeta^i}{\partial u_i} \\ \frac{\partial \eta^i}{\partial v_i} & \frac{\partial \zeta^i}{\partial v_i} \end{vmatrix}; B_i = \begin{vmatrix} \frac{\partial \zeta^i}{\partial u_i} & \frac{\partial \xi^i}{\partial u_i} \\ \frac{\partial \zeta^i}{\partial v_i} & \frac{\partial \xi^i}{\partial v_i} \end{vmatrix}; \ C_i = \begin{vmatrix} \frac{\partial \xi^i}{\partial u_i} & \frac{\partial \eta^i}{\partial u_i} \\ \frac{\partial \xi^i}{\partial v_i} & \frac{\partial \eta^i}{\partial v_i} \end{vmatrix}.$$

The tangential component of reaction force, i.e. the friction force, is comprised in the tangent plane at the support surface. The equation of the tangent plane in the point P^i (ξ_{Pi}, η_{Pi}, ζ_{Pi}) is

$$\begin{vmatrix} \xi^i - \xi_{Pi} & \eta^i - \eta_{Pi} & \zeta^i - \zeta_{Pi} \\ \frac{\partial \xi^i}{\partial u_i} & \frac{\partial \eta^i}{\partial u_i} & \frac{\partial \zeta^i}{\partial u_i} \\ \frac{\partial \xi^i}{\partial v_i} & \frac{\partial \eta^i}{\partial v_i} & \frac{\partial \zeta^i}{\partial v_i} \end{vmatrix} = 0,$$

or: $\xi^i A_i + \eta^i B_i + \zeta^i C_i - \xi_{Pi} A_i - \eta_{Pi} B_i - \zeta_{Pi} C_i = 0$.

The straight-line support of the friction force is included in the tangent plane:

$$\frac{\xi^i - \xi_{Pi}}{l_i} = \frac{\eta^i - \eta_{Pi}}{m_i} = \frac{\zeta^i - \zeta_{Pi}}{n_i},$$

therefore: $A_i l_i + B_i m_i + C_i n_i = 0$.

If the surface over which the robot walked is plane, it is possible that the robot may slip to the direction of the maximum slope.

Generally, the sliding result is a rotational motion superposed on a translational one. The instantaneous axis has an unknown position.

Let us consider

$$\frac{\xi - U}{\cos \alpha_r} = \frac{\eta - V}{\cos \beta_r} = \frac{\zeta}{\cos \gamma_r}$$

the equation of instantaneous axis under canonical form, with respect to the fixed coordinate axes system The components of speed of the point P^i, on the fixed coordinate axes system with OZ axis identical with the instantaneous axis, are:

$$\overline{V}_X = -\omega Y\bar{i};\ \overline{V}_Y = \omega X\bar{j};\ \overline{V}_Z = \overline{V}_0,$$

The projections of the P^i point speed on the axes of fixed system $O\xi\eta\zeta$ are:

$$\begin{Vmatrix} V_\xi \\ V_\eta \\ V_\varsigma \end{Vmatrix} = \mathbf{R} \begin{Vmatrix} V_X \\ V_Y \\ V_Z \end{Vmatrix},$$

where **R** is the matrix of rotation in space.

The carrier straight line of P^i point speed, i.e. of the tangential component of reaction force, has the equations

$$\frac{\xi - \xi_{Pi}}{V_\xi} = \frac{\eta - \eta_{Pi}}{V_\eta} = \frac{\zeta}{V_\zeta},$$

and is contained in the tangent plane to the terrain surface in the point P^i:

$$V_\xi l + V_\eta m + V_\zeta n = 0.$$

To determine the stable position of the walking robot which leans upon n legs, on some shape terrain, it is necessary to solve a nonlinear system, which is formed by:

- the transformation matrix equation

$$\begin{Vmatrix} 1 \\ X_{0Pi} \\ Y_{0Pi} \\ Z_{0Pi} \end{Vmatrix} = \mathbf{A}\mathbf{A}_0^i\mathbf{A}_1^i\mathbf{A}_2^i\mathbf{A}_3^i \begin{Vmatrix} 1 \\ X_{4Pi} \\ Y_{4Pi} \\ Z_{4Pi} \end{Vmatrix},$$

where:

A is the transformation matrix of coordinate of a point from the system $O_0X_0Y_0Z_0$ of the robot platform to the system $O\xi\eta\zeta$;

$\mathbf{A}_i$ is the Denavit – Hartenberg transformation matrix of coordinates of a point from the system $O_{i+1}X_{i+1}Y_{i+1}Z_{i+1}$ of the element (***i***) to the system $O_iX_iY_iZ_i$ of the element (***i*-1**) (Denavit J. & Hartenberg R.S., 1955), (Uicker J.J.jr., Denavit J., Hartenberg R.S., 1965):

- the balance equations

$$\sum_{i=1}^{n} \overline{R}_i + \overline{F} = 0; \ \sum_{i=1}^{n} \overline{M}_{(R_i)} + \overline{M} = 0, \tag{8}$$

which expressed the equilibrium of the forces and moments system, which acted on the elements of walking robot.

The $\overline{F}$ and $\overline{M}$ are the wrench components of the forces and moments which represent the robot load, including the own weight.

The unknowns of the system are:

- the coordinates X_T, Y_T, Z_T and direction cosines cos α_T, cos β_T, cos γ_T which define the platform position with respect to the terrain:
- the normal $\overline{N}_i$ and the tangential $\overline{T}_i$, $i = \overline{1,n}$, components of the reaction forces;
- the direction numbers l_i, m_i, n_i, $i = \overline{1,n}$, of the tangential components;
- the position parameters U, V, cos α, cos β, cos γ of the instantaneous axis;
- the magnitude of the V_0 / ω ratio, where V_0 is the translational instantaneous speed of the hardening structure (Okhotsimski D.E. & Golubev I., 1984). The system is compatible for $n = 3$ support points.

If the number of feet which are simultaneous in the support phase is larger than three the system is undetermined static and is necessary to take into consideration the deformations of the mechanical structure of the walking robot and terrain. In case of a quadrupedal walking robot, the hardening configuration is a six fold hyperstatical structure. To determinate the force distribution, one must use a specific method for indeterminate static systems.

The canonical equations in stress method are (Buzdugan Gh., 1980):

$$\begin{aligned} &\delta_{11}\, x_1 + \delta_{12}\, x_2 + \ \ldots + \delta_{16}\, x_6 = \ -\delta_{10}; \\ &\delta_{21}\, x_1 + \delta_{22}\, x_2 + \ \ldots + \delta_{26}\, x_6 = \ -\delta_{20}; \\ &\ldots\ldots \end{aligned} \tag{9}$$

$$\delta_{61}\, x_1 + \delta_{62}\, x_2 + \ \ldots + \delta_{66}\, x_6 = \ - \delta_{60};$$

where:

δ_{ij} is the displacement along the O_iX_i direction of stress owing to unit load which acts on the direction and in application point of the O_iX_j;

δ_{i0} is the displacement along the X_i direction of stress owing to the external load when $O_iX_j = 0,\ i = \overline{1,6}$:

$$\delta_{i0} = \sum_{p=1}^{4} \int \frac{M_{y0} m_{yi}}{EI_{y1}} \mathrm{d}x + \sum_{q=1}^{4} \int \frac{M_{y0} m_{yi}}{EI_{y2}} \mathrm{d}x, i = \overline{1,6};$$

$$\delta_{ij} = \sum_{p=1}^{4} \int \frac{M_{xi} m_{xi}}{GI_{x1}} \mathrm{d}x + \sum_{q=1}^{4} \int \frac{M_{xi} m_{xi}}{GI_{x2}} \mathrm{d}x +$$

$$+ \sum_{q=1}^{4} \int \frac{M_{xi} m_{xi}}{GI_{x3}} \mathrm{d}x + \sum_{p=1}^{4} \int \frac{M_{yi} m_{yi}}{GI_{y1}} \mathrm{d}x +$$

$$+ \sum_{q=1}^{4} \int \frac{M_{yi} m_{yi}}{GI_{y2}} \mathrm{d}x + \sum_{q=1}^{4} \int \frac{M_{yi} m_{yi}}{GI_{y3}} \mathrm{d}x +$$

$$+ \sum_{p=1}^{4} \int \frac{M_{zi} m_{zi}}{GI_{z1}} \mathrm{d}x + \sum_{q=1}^{4} \int \frac{M_{zi} m_{zi}}{GI_{z2}} \mathrm{d}x +$$

$$+ \sum_{q=1}^{4} \int \frac{M_{zi} m_{zi}}{GI_{z3}} \mathrm{d}x, \quad i = \overline{1,6}, j = \overline{1,6};$$

$GI_{xi},\ i = \overline{1,3}$, are the torsion stiffness of the legs elements lowers, middles and uppers respectively;

EI_{yi} and $EI_{zi},\ i = \overline{1,3}$, are the bend stiffness of the legs elements lowers, middles and uppers respectively;

M are the bending moments in basic system which is loaded with basic charge;

m are the bending moments in the basic system loaded with the unit charge.

The definite integrals

$$I = \int_a^b M m \mathrm{d}x$$

are calculated by the Simpson method:

$$I = \frac{b-a}{6}[(M_a + M_b)(m_a + m_b) + M_a m_a + M_b m_b].$$

To calculate the m_{xi}, m_{yi}, m_{zi}, M_{xi}, M_{yi}, $M_{zi},\ i = \overline{1,6}$, seven systems are used (Fig. 8), namely:

- the system S_0, where the single load is G, and $X_i = 0,\ i = \overline{1,6}$;

- the systems S_i, where the single load is $X_i = 1,\ i = \overline{1,6}$.

The remaining unknowns, namely $x_i,\ i = \overline{7,\ 12}$, are calculated from the equations (9). The normal and tangential components of the reaction forces are calculated as function of the positions of tangent planes on the terrain surface at the support points.
The following hypotheses are considered as true:

- the stiffnesses of the legs are much less than the robot's platform stiffness;
- the four legs are identically.
- the cross sections of the leg's elements are constant.

In Fig. 9, a modular walking robot with six legs is shown. The hardening structure of this robot is a 12-fold hyperstatical structure.

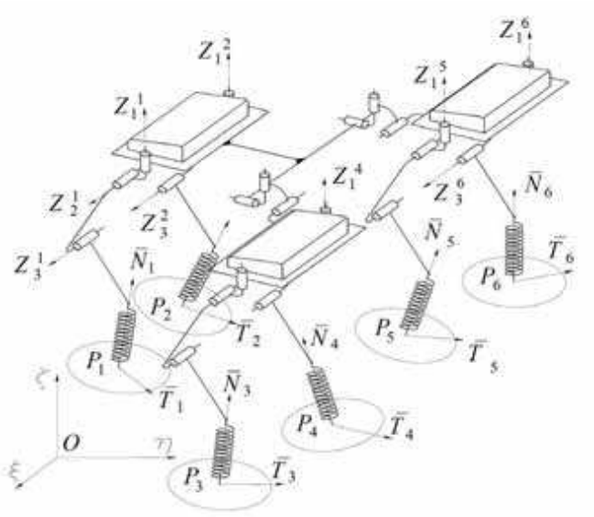

Fig. 9. The reaction force components in the support points of the modular walking robot

5. Movement of Walking Robots

Part of the characteristic parameters of the walking robot may change widely enough when using it as a transportation mean. For instance, the additional loads on board, change the positions of the gravity centers and the inertia moments of the module's platforms. Environmental factors such as the wind or other elements may bias the robot, and their influence is barely predictable. Such disturbances can cause considerable deviations in the real movement of the robot than expected.
Drawing up and using efficient methods of finding out the causes of such deviations, as well as of avoiding such causes, represent an appropriate way of enhancing the walking robot's proficiency and this at lower power costs.

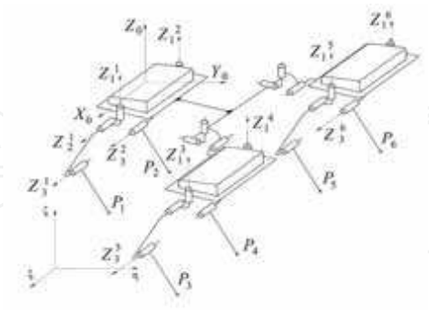

Fig. 10. Kinematics scheme of walking modular robot

Working out and complete enough mathematical pattern for studying the movement of a walking robot is interesting, both as regards the structure of its control system and verifying the simplifying principles and hypotheses, that the control program's algorithms rely on. The static stability issue is solved by calculating the positions of each foot against the axes system, attached to the platform, and whose origin is in the latter's gravity center (Waldron K.J. 1985).

The static stability of the gait is a problem which appears on the quadrupedal walking robot movement.

When a leg is in the transfer phase, the vertical projection of the gravity center of the hardening structure may be outside of the support polygon, i.e. support triangle. It is the case of the walking robot made by two modules. The gait 3×3 (Song S.M. & Waldron K.J., 1989), (Hirose S., 1991) of the six legged walking robot, made by three modules, is static stable (Fig. 10). S. Hirose defined the *stability margin*s that are the limits distances between the vertical projection of the gravity center and the sides of the support triangle. To provide the static stability of the quadrupedal walking robots two methods are used:

- the waved gait,
- the swinging gait.

In the first case, before a leg is lifted up the terrain, all leg are moved so that the robot platform to be displaced in the opposite side to the leg that will be lifted. In this way, the vertical projection of the gravity center moved along a zigzag line.

In the second case, before a leg is lifted, this is extended and the diagonal-opposite leg is compressed.

So, the robot platform has a swinging movement, and the vertical projection of the gravity center also has a zigzag displacement. This gait can not be used if the robot load must be hold in horizontal position.

The length of the step does not influence the limits of the static stability of the walking robot because the mass of a leg is more less than mass of the platform.

A walking robot, which moves under dynamical stability condition can attain higher velocities and can make steps with a greater length and a greater height. But, the central platform of the robot cannot be maintained in the horizontal position because it tilted to the foot which is lifted off the terrain. The size of the maximum inclination angle depends to the forward speed of the walking robot.

The stability problem is very important at the moving of the quadrupedal walking robots. When a foot is lifted off the terrain and the other legs supporting the robot's platform are in contact with the terrain. If the vertical projection G' of the gravity center G of the legged robot is outside of the supporting polygon (triangle P^1 P^2 P^3, Fig. 11), and the cruising speed is greater than a certain limit, the movement of the robot happens under condition of the dynamical stability. When the leg (**4**) is lifted off the terrain, the walking robot rotates around of the straight line which passing through the support points P^2 and P^3.

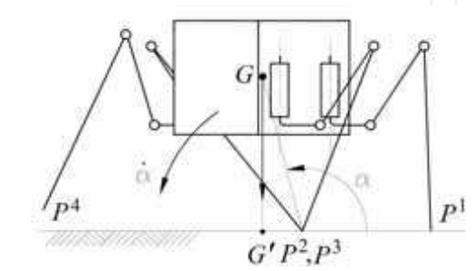

Fig. 11. The overturning movement of the walking robot

The magnitude of the forward speed did not influence the rotational motion of the robot around the straight line P^2P^3. This rotational motion can be investigated with the Lagrange's equation (Appel P. 1908):

$$\frac{\mathrm{d}}{\mathrm{d}t}\left(\frac{\partial T}{\partial \dot{q}}\right) - \frac{\partial T}{\partial q} + \frac{\partial P}{\partial q} = Q \tag{10}$$

The kinetic and potential energies of the hardening configuration of the robot have the forms

$$T = (m\,AG^2 + I)\frac{\dot{\alpha}^2}{2},\; P = m\,g\,AG(1-\sin\alpha), \tag{11}$$

and the generalized force is

$$Q = -m\,g\,AG\cos\alpha. \tag{12}$$

where m denotes the mass of the entire robot, I is the moment of inertia of the robot structure with respect to the axis passed by G and AG is the distance between the gravity center G and the rotational axis P^2P^3 ($\alpha > \pi/2$) (Fig. 11).

Substituting the (11) and (12) into (10), it results

$$\ddot{\alpha} = -\frac{2m\,g\,AG\cos\alpha}{I + m\,AG^2} \tag{13}$$

Because the moment of inertia of a body is proportional with its mass, the angular acceleration $\ddot{\alpha}$ does not dependent on the mass m.

The quadrupedal walking robot in question, which moved so that the step size is 0.2 m, with forward average speed equal to 3.63 m/s (13 km/h approximate) has the maximum inclination of the platform equal to 0.174533. This forward speed is very great for the usual applications of the walking robots. As a result, the movement of the legged robots is made under condition of the static stability. The conventional quadrupedal walking robots have

rather sluggish gaits for walking, but are unable to move smoothly and quickly like animal beings.

6. Optimization of Kinematic Dimension of Displacement Systems of Walking Robots

For the walking robot to get high shift performances on an as different terrain configurations as possible, and for increasing the robot's mobility and stability, under such circumstances, it is required a very careful survey on the trajectory's control, which involves both to determine the coordinates of the feet's leaning points, as related to the robot's body, and the calculation of the platform's location during the walking, as against a set system of coordinates in the field.

These performances are closely connected with the shift system's structure and the dimensions of the compound elements. For simplifying its mounding, it is accepted the existence of a point-shaped contact between the foot and the leaning area.

The shift system mechanism of any walking robot is built so that he could achieve a multitude of the toes' trajectories. These courses may change according to the ground surface, at every step. Choosing a certain trajectory depends on the topography of the surface that the robot is moving on. As one could already notice, during time, the shift mechanism is the most important part of the walking robot and it has one or several degrees of freedom, contingent of the kinematics chain that its structure relies on.

Considering the fact that the energy source is fixed on the robot's platform, the dimensions of the legs mechanism's elements are calculated using a multicritical optimization proceeding, which includes several restrictions. The objective function (Fox R. 1973), (Goldberg D. 1999), (Coley D. 1999) may express:

- the mechanical work needed for shifting the platform by one step ;
- the maximum driving force needed for the leg mechanism;
- the maximum power required for shifting, and so on.

These objective functions can be considered separately or simultaneously. The minimization of the mechanical work consumed for defeating of the friction forces can be considered in the legs mechanisms' synthesis also by a multicritical optimization.

The kinematics dimensions of the shift system mechanism elements are obtained as a result of several considerations and calculation taking into account the degree of freedom, the energy consumption, the efficiency, the kinematics performances, the potential distribution, the operation field and the movement regulating algorithm.

There are two possibilities in order to decrease the energy consumption of a walking robot. One of then is to optimize the shifting system of the robot. That could be performing by the kinetostatic synthesis of the leg mechanism with minimization of energy consumption during a stepping cycle.

A second possibility to decrease the energy consumption is the static balancing of the leg mechanism [Ebert-Uphoff I. & Gosellin C.M. 1998), (Ion I., Simionescu I. & Ungureanu M. 2001), (Simionescu I. & Ion I.2001).

The energy consumption is especially depended on the moving law of the platform, which has the biggest mass.

The simplest constructional solution for the leg mechanisms of the walking robot uses the revolute pairs only. The linear hydraulic motor has only a prismatic pair (Fig. 12). This

mechanism consists of two plane kinematics chains. One of these kinematics chains is composed by the links (**1**), (**2**) and (**3**), and operated in the horizontal plane. The other kinematics chain operated in the vertical plane and is formed by the elements (**4**), (**5**), (**6**), (**7**), (**8**) and (**9**). The lengths of the elements (**6**) and (**7**), i.e. the distances *IH* and *HP* respectively, are calculated in terms of the size of the field in which the *P* point of the low end of the leg is displaced. The magnitudes of the driving forces F_{d2} between the piston (**5**) and the cylinder (**4**) and F_{d1} between the piston (**8**) and the cylinder (**9**) are calculated with the following relations:

$$F_{d1} = \frac{Q_x(Y_H - Y_P) - Q_y(X_H - X_P)}{(X_H - X_L)\sin\varphi_2 - (Y_H - Y_L)\cos\varphi_2} + \\ + \frac{(m_7 + m_8)g(X_H - X_L) - m_7 g(X_{G7} - X_L)}{(X_H - X_L)\sin\varphi_2 - (Y_H - Y_L)\cos\varphi_2}; \tag{14}$$

$$F_{d2} = \frac{R_{69Y}(X_I - X_J) + R_{67Y}(X_I - X_H)}{(X_H - X_L)\sin\varphi_2 - (Y_H - Y_L)\cos\varphi_2} + \\ + \frac{(m_5 + m_6)g(X_I - X_G) - m_6 g(X_{G6} - X_G)}{(X_H - X_L)\sin\varphi_2 - (Y_H - Y_L)\cos\varphi_2} + \\ + \frac{R_{69X}(Y_I - Y_J) - R_{67X}(Y_I - Y_H)}{(X_H - X_L)\sin\varphi_2 - (Y_H - Y_L)\cos\varphi_2}, \tag{15}$$

where:

$$R_{69X} = F_{d1}\cos\varphi_2;$$
$$R_{69Y} = F_{d1}\sin\varphi_2 + m_9 g;$$
$$R_{67X} = -Q_X - F_{d1}\cos\varphi_2;$$
$$R_{67Y} = (m_7 + m_8 + m_9)g - Q_Y - F_{d1}\sin\varphi_2;$$
$$\varphi_1 = \arctan\frac{Y_G - Y_E}{X_G - X_E};$$
$$\varphi_2 = \arctan\frac{Y_L - Y_J}{X_L - X_J}.$$

The m_i, X_{Gi} and Y_{Gi} represent the mass and the coordinates of gravity centre of element (***i***) respectively.

The mechanical work of the driving forces F_{d1} and F_{d2}, performed in the *T* time when the robot platform advances with a step by one single leg, has the form:

$$W = \int_0^T (F_{d1}\frac{\mathrm{d}JL}{\mathrm{d}t} + F_{d2}\frac{\mathrm{d}EG}{\mathrm{d}t})\mathrm{d}t, \tag{16}$$

where:

$$\frac{\mathrm{d}EG}{\mathrm{d}t} = \frac{1}{EG}\left[(X_G - X_E)\frac{\mathrm{d}X_G}{\mathrm{d}t} + (Y_G - Y_E)\frac{\mathrm{d}Y_G}{\mathrm{d}t}\right];$$

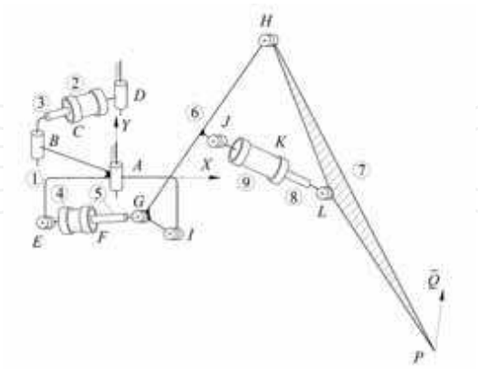

Fig. 12. Mechanism of leg

$$\frac{\mathrm{d}JL}{\mathrm{d}t} = \frac{1}{JL}\left[(X_L - X_J)(\frac{\mathrm{d}X_L}{\mathrm{d}t} - \frac{\mathrm{d}X_J}{\mathrm{d}t}) + \right.$$

$$\left. + (Y_L - Y_J)(\frac{\mathrm{d}Y_L}{\mathrm{d}t} - \frac{\mathrm{d}Y_J}{\mathrm{d}t})\right];$$

$$EG = \sqrt{(X_G - X_E)^2 + (Y_G - Y_E)^2};$$

$$JL = \sqrt{(X_L - X_J)^2 + (Y_L - Y_J)^2};$$

$$X_G = X_I + GI\cos(\varphi_{IH} + \beta);$$

$$Y_G = Y_I + GI\sin(\varphi_{IH} + \beta);$$

$$X_L = X_P + PL\cos(\varphi_{PH} + \alpha);$$

$$Y_L = Y_P + PL\sin(\varphi_{PH} + \alpha);$$

$$\alpha = \arccos\frac{HP^2 + LP^2 - HL^2}{2HP \cdot LP};$$

$$\beta = \arccos\frac{HI^2 + GI^2 - GH^2}{2HI \cdot GI};$$

$$\varphi_{IH} = \arccos\frac{V_1\sqrt{U_1^2 + V_1^2 - W_1^2} - U_1W_1}{U_1^2 + V_1^2},$$

$$U_1 = 2HP(X_P - X_H),\ V_1 = 2HP(Y_P - Y_H),$$

$$W_1 = HP^2 + (X_P - X_I)^2 + (Y_P - Y_I)^2 - HI^2,$$

$$\varphi_{IH} = \arccos\frac{V_2\sqrt{U_2^2 + V_2^2 - W_2^2} - U_2W_2}{U_2^2 + V_2^2},$$

$$U_2 = 2HI(X_I - X_H),\ V_2 = 2HI(Y_I - Y_H),$$

$$W_2 = HI^2 + (X_P - X_I)^2 + (Y_P - Y_I)^2 - HP^2;$$

$$\frac{d\varphi_{IH}}{dt} = \frac{HI}{E}\left(\frac{dY_P}{dt}\sin\varphi_{PH} + \frac{dX_P}{dt}\cos\varphi_{PH}\right);$$

$$\frac{d\varphi_{PH}}{dt} = \frac{PI}{E}\left(\frac{dY_P}{dt}\sin\varphi_{IH} + \frac{dX_P}{dt}\cos\varphi_{IH}\right)$$

$$E = HP \cdot HI\sin(\varphi_{IH} - \varphi_{PH}) \neq 0.$$

The minimization of the mechanical work of the driving forces is done with constrains which are limiting the magnitudes of the transmission angles of the forces in the leg mechanism, namely:

$$R_1 = \Psi - \delta_{\min} \geq 0;\ R_2 = \delta_{\max} - \Psi \geq 0; \tag{17}$$

$$R_3 = \Theta - \delta_{\min} \geq 0;\ R_4 = \delta_{\max} - \Theta \geq 0; \tag{18}$$

and the magnitude of the Θ angle between the vectors $\overline{HI}$ and $\overline{HP}$. This angle depends on the maximum height of the obstacle over which the walking robot can passes over, and on the maximum depth of the hallows which it may be stepped over:

$$R_5 = \Phi - \lambda_{\min} \geq 0;\ R_6 = \lambda_{\max} - \Phi \geq 0, \tag{19}$$

where: $\Psi = \varphi_{IH} - \beta - \arctan\frac{Y_G - Y_E}{X_G - X_E}$;

$$\Theta = \varphi_{PH} + \arccos\frac{HL^2 + HP^2 - LP^2}{2HL \cdot HP} - \arctan\frac{Y_J - Y_L}{X_J - X_L};$$

$$\Phi = \varphi_{HP} - \varphi_{IH}.$$

The Ψ angle is measured between the vectors $\overline{GI}$ and $\overline{GE}$. The dimensions *HI*, *HP*, *LP*, *HG*, *IJ*, *JH*, α and β of the elements and the coordinates X_E, Y_E X_I, Y_I, of the fixed points *E* and *I* are considered as the unknowns of the synthesis problem.

The necessary power for acting the leg mechanism is calculated by the relation

$$P = F_{d1}\frac{dEG}{dt} + F_{d2}\frac{dJL}{dt}. \tag{20}$$

The maximum power value is minimized in the presence of the constrains (17), (18) and (19).

7. Static Balancing of Displacement Systems of Walking Robots

The walking robots represent a special category of robots, characterized by having the power source embarked on the platform. This weight of this source is an important part of the total charge that the walking machine can be transported. That is the reason why the walking system must be designed so that the mechanical work necessary for displacement, or the highest power necessary to act it, should be minimal. The major energy consumption of a walking machine is divided into three different categories:

- the energy consumed for generating forces required to sustain the platform in gravitational field; in other word, this is the energy consumed to compensate the potential energy variation;

- the energy consumed by leg mechanism actuators, for the walking robot displacement in acceleration and deceleration phases;
- the energy lost by friction forces and moments in kinematics pairs.

The magnitude of reaction forces in kinematics pairs and the actuator forces depend on the load distribution on the legs. For slow speed, joint gravitational loads are significantly larger than inertial loads; by eliminating gravitational loads, the dynamic performances are improved.

Therefore, the power consumption to sustain the walking machine platform in the gravitational field can be reduced by using the balancing elastic systems and by optimum design of the leg mechanisms. The potential energy of the walking machine is constant or has a little variation, if the static balance is achieved. The balancing elastic system consist of by rigid and linear elastic elements.

7.1 Synthesis of Static Balancing Elastic Systems

The most usual constructions of the leg mechanisms have three degree of freedom. The proper leg mechanism is a plane one and has two degree of freedom (Fig. 13). This mechanism is articulated to the platform and it may be rotated around a vertical axis. To reduce the power consumption by robot driving system it is necessary to use two balancing elastic systems. One must be set between links (**2**) and (**3**), and the other - between links (**3**) and (**4**). Because the link (**3**) is not fixed, the second balancing elastic system can not be set. Therefore, the leg mechanism schematized in Fig. 13 can be balanced partially only (Streit, D.,A. & Gilmore, B.,J. , 1989).

It is well known and demonstrated that the weight force of an element which rotate around a horizontal fixed axis can be exactly balanced by the elastic force of a linear helical spring (Simionescu I. & Moise V. 1999). The spring is jointed between a point belonging to the element and a fixed one. The major disadvantage of this simple solution is that the spring has a zero undeformed length. In practice, the zero free length is very difficult to achieve or even impossible. The opposite assertions are theoretically conjectures only. A zero free length elastic device comprised a compression helical spring. In the construction of this device, some difficulties arise, because the compression spring, corresponding to the calculated feature, must be prevented from buckling. A very easy constructive solution, which the above mentioned disadvantage is removed, consists in assembly two parallel helical springs, as show in Fig. 13. The equilibrium of forces which act on the link (**3**) is expressed by following equation:

$$(m\,BC\cos\varphi_{3i} - m_{7F}\,X_F - m_{8I}\,X_I - m_2\,X_{G2})g - F_{s7}\,BF\sin$$
$$(\varphi_{3i} - \psi_{1i} + \alpha_1) - F_{s8}\,BI\sin(\varphi_{3i} - \psi_{2i} + \alpha_2) = 0,\ i = \overline{1,12}\,, \tag{21}$$

where:

m is the mass of distributed load on leg in the support phase, including the mass of the link (**2**) and the masses of linear helical springs (**7**) and (**8**), concentrated at the points H and J respectively;

m_{7F} and m_{8I} are the masses of springs (**7**) and (**8**), concentrated at the points F and I respectively;

$$\psi_{1i} = \arctan\frac{Y_{F_i} - Y_H}{X_{F_i} - X_H};\ \psi_{2i} = \arctan\frac{Y_{I_i} - Y_J}{X_{I_i} - X_J};$$

$$X_{F_i} = BF\cos(\varphi_i + \alpha_1);\ Y_{F_i} = BF\sin(\varphi_i + \alpha_1);$$

$$X_{I_i} = BI\cos(\varphi_i + \alpha_2);\ Y_{I_i} = BI\sin(\varphi_i + \alpha_2);$$

$$F_{s7} = F_{07} + k_7(HF_i - l_{07});\ F_{s8} = F_{08} + k_8(JI_i - l_{08});$$

$$\alpha_1 = \arctan\frac{y_{3F}}{x_{3F}};\ \alpha_2 = \arctan\frac{y_{3I}}{x_{3I}};$$

$$HF_i = \sqrt{(X_H - X_{F_i})^2 + (Y_H - Y_{F_i})^2};$$

$$JI_i = \sqrt{(X_J - X_{I_i})^2 + (Y_J - Y_{I_i})^2}.$$

The equations (21), which are written for twelve distinct values of the position angles φ_{3i}, are solved with respect to following unknowns: x_{3F}, y_{3F}, x_{3I}, y_{3I}, X_H, Y_H, X_J, Y_J, F_{07}, F_{08}, l_{07}, l_{08}. The undeformed lengths l_{07} and l_{08} of the springs given with acceptable values from constructional point of view.

The masses m, m_1, m_2, m_7, m_8 of elements and springs, and the position of the gravity center G_2 are assumed as knows. In fact, the problem is solved in an iterative manner, because at the start of the design, the masses of springs are unknowns.

The angles φ_{3i} must be chosen so that, in the positions which correspond to the support phase, the loading of the leg is full, and in the positions which correspond to the transfer phase, the loading is null. The static balancing is achieved theoretical exactly in the positions defined by angles φ_{33i}, $i = \overline{1,12}$. Between these positions, the unbalancing is very small and may be neglected.

If a total statically balancing is desired, a more complicated leg structure is necessary to used. In the mechanism leg schematized in Fig. 14, the two active pairs are superposed in B. The second balancing elastic system is set between the elements (**2**) and (**5**).

The equilibrium equation of forces which act on the elements (**3**) and (**5**) respectively are:

$BC(R_{34Y}\cos\varphi_{3i} - R_{34X}\sin\varphi_{3i}) + (m_{7F}X_F + m_{8I}X_I + m_3 X_{G3})g + F_{s7}\,BF\sin(\varphi_{3i} - \varphi_{7i} + \alpha_1) + F_{s8}\,BI\sin(\varphi_{3i} - \varphi_{8i} + \alpha_2) = 0;$

$BE(R_{56Y}\cos\varphi_{5i} - R_{56X}\sin\varphi_{5i}) + (m_{9N}X_N + m_{10L}X_L + m_5 X_{G5})g + F_{s9}\,BN\sin(\varphi_{5i} - \varphi_{9i}) + \alpha_3) + F_{s10}\,BL\sin(\varphi_{5i} - \varphi_{10i} + \alpha_4) = 0,\ i = \overline{1,12}$,

where: $\alpha_3 = \arctan\frac{y_{5N}}{x_{5N}};\ \alpha_4 = \arctan\frac{y_{5L}}{x_{5L}};$

$$F_{S9} = F_{09} + k_9(ML_i - l_{09});\quad F_{S10} = F_{0,10} + k_{10}(QN_i - l_{0,10});$$

$$R_{34X} = \frac{U(X_D - X_E) - V(X_C - X_D)}{W};$$

$$R_{34Y} = \frac{V(Y_D - Y_C) - U(Y_E - Y_D)}{W};$$

$$U = g[m_4(X_{G4} - X_D) - m(X_P - X_D)];$$

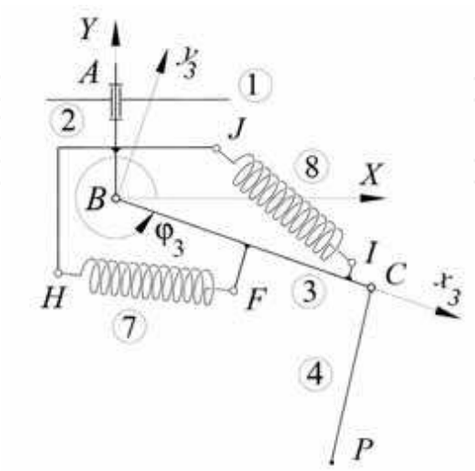

Fig. 13. Elastic system for the discrete partial static balancing of the leg mechanism

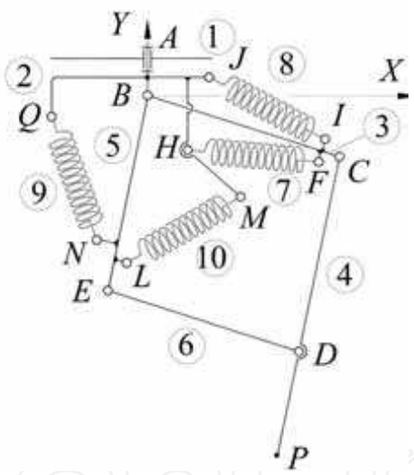

Fig.14 Elastic system for the discrete total static balancing of the leg mechanism

$$V = g[m_6(X_{G6} - X_D) - (m_4 - m_6 - m)(X_E - X_D)];$$
$$W = Y_D(X_C - X_E) - Y_C(X_D - X_E) - Y_E(X_C - X_D);$$
$$R_{56X} = -R_{34X};\ R_{56Y} = (m_4 + m_6 - m)g - R_{34Y}.$$

The magnitudes of the angles φ_{3i} and φ_{5i} are calculated as functions on the position of the point *P*. The variation fields of these, in support and transfer phase, must not be intersected. In the support phase, the point *P* of the leg is on the terrain. In the return phase, the leg is not on the terrain, and the distributed load on the leg is zero. The not intersecting condition can be easy realized for the variation fields of angle φ_3. If the working positions of link (**4**)

are chosen in proximity of vertical line, the driving force or moment in the pair *C* is much less than the driving force from the pair *B*. This is workable by the adequately motions planning. In this manner, the diminishing of energy consumed for the walking machine displacement can be made by using the partial balancing of leg mechanism only.

The static balancing is exactly theoretic realized in twelve positions of the link (**3**), accordingly to the angle values φ_{3i}, $i = \overline{1,12}$, only. Due to continuity reasons, the unbalancing magnitude between these positions is negligible.

In order to realize the theoretic exactly static balancing of the leg mechanism, for all positions throughout in the work field, it is necessary to use the cam mechanisms. In Fig. 15 is shown a elastic system for continuous balancing, consist of a helical spring (**7**), jointed on the link (**3**) and the follower (**8**), which slides along the link (**2**). The cam which acted the follower, by the agency of role (**9**), is fixed on the link (**3**). The parametrical equations of directrices curves of the cam active surface are:

$$x_2 = Y_D \sin\varphi_3 \mp \frac{R\left(\frac{dY_D}{d\varphi_3}\cos\varphi_3 - Y_D \sin\varphi_3\right)}{P};$$

$$y_2 = Y_D \cos\varphi_3 \pm \frac{R\left(\frac{dY_D}{d\varphi}\sin\varphi_3 + Y_D \cos\varphi_3\right)}{P},$$

where *R* represents the role radius, and:

$$P = \sqrt{\left(\frac{dY_D}{d\varphi_3}\right)^2 + Y_D^2},$$

The ordinate Y_D of point *D* and its derivative $\frac{dY_D}{d\varphi_3}$ are calculated as solutions of following differential equation which expressed the equilibrium condition of force system which are taken into consideration:

$$g(BC\, m + m_3 BG_3 + BF\, m_{7F})\cos\varphi_3 + F_{s7}\, BF \sin(\varphi_3 - \psi) + Y_D\, R_{93} \sin\alpha = 0, \tag{22}$$

where the reaction force R_{93} between cam (**3**) and role (**9**) has the expression:

$$R_{93} = [F_{s7} \sin\psi + (m_8 + m_9 + m_{7F})\, g] \cdot \frac{P}{Y_D},$$

and: $X_F = BF\cos\varphi_3$; $Y_F = BF\sin\varphi_3$;

$$X_H = 0;\ Y_H = Y_D - DH;$$

$$\alpha = \arctan\frac{\frac{dY_D}{d\varphi_3}}{Y_D};\ \psi = \arctan\frac{Y_H - Y_F}{-X_F};$$

$$F_{s7} = F_{07} + k_7 (FH - l_{07});$$

$$FH = \sqrt{(X_F - X_H)^2 + (Y_F - Y_H)^2}$$

The mass m_7 of the helical spring (7) is assumed as concentrated in joints H and F, m_{7F} and m_{7H} respectively. The masses m, m_1, m_2, m_3 and m_4 of the bodies, dimensions BF, BC, DH and helical spring characteristics F_{07}, l_{07} and, k_7 are considered knows.

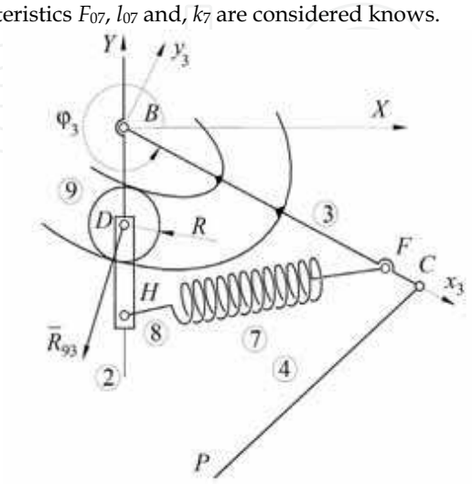

Fig.15. Elastic system for the continuous partial static balancing of the leg mechanism VARIANT I

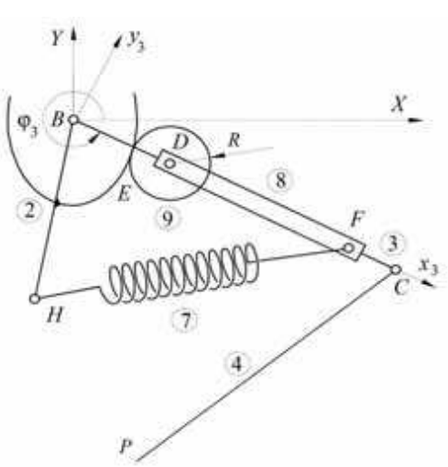

Fig.16. Elastic system for the continuous partial, static balancing of the leg mechanism VARIANT II

The initial conditions, which are necessary to integrate the differential equation (22) are considered in a convenient mode, adequate to a known equilibrium position.

In Fig. 16 is schematized another elastic system for continuous balancing. The balancing helical spring (7) is jointed with an end to the follower (8) at the point F, and with the other

one to link (**2**), at point *H*. The cam is fixed to the link (**2**). The follower (**8**) slid along the link (**3**). The parametrical equations of directrice curves of the cam active surface are:

$$x_2 = X_D \mp \frac{R\left(\frac{\mathrm{d}BD}{\mathrm{d}\varphi_3}\sin\varphi_3 + X_D\right)}{Q},$$

$$y_2 = Y_D \pm \frac{R\left(\frac{\mathrm{d}BD}{\mathrm{d}\varphi_3}\cos\varphi_3 - Y_D\right)}{Q},$$

where: $X_D = BD\cos\varphi_3$, $Y_D = BD\sin\varphi_3$, and $Q = \sqrt{\left(\frac{\mathrm{d}X_D}{\mathrm{d}\varphi_3}\right)^2 + \left(\frac{\mathrm{d}Y_D}{\mathrm{d}\varphi_3}\right)^2}$.

The distance *BD* and its derivative $\frac{\mathrm{d}BD}{\mathrm{d}\varphi_3}$ are calculated as solutions of following differential equation

$$F_{s7}\frac{Y_H(BD+DF)\cos\varphi_3}{FH} - R_{29}BD\cos(\varphi_3-\alpha) - g(m_3BG_3 + \\ + m_{4A}(BD+DF) + m_8(BD+DG_8))\cos\varphi_3 = 0, \tag{23}$$

where:

$$R_{29} = \frac{g(m_8 + m_9 + m_{7F}) - F_{s7}\cos(\varphi_3 - \psi)}{\cos(\varphi_3 - \alpha)};$$

$$\alpha = \arctan\frac{\frac{\mathrm{d}BD}{\mathrm{d}\varphi_3}}{BD}.$$

8. Design of Foot Sole for Walking Robots

The feet of the walking robots must be build so that the robots are able to move with smooth and quick gait. If the fact soles were not shaped to fit with the terrain surface, then the foot would not be able to apply necessary driving forces and the resulting gait were not uniform. In a simplified form, the leg of a legged walking anthropomorphous robot is build of three parts (Fig. 17), namely thigh (**1**), shank (**2**) and foot (**3**). All of the joint axes are parallel with the support plane of the land. The legged robot foot soles have curved front and rear ends, corresponding to the toes tip and to the heel respectively. If the position of the axis of the pair *A* is defined with respect to the fixed coordinate axes system fastened on the support plane, the leg mechanism has a degree of freedom in the support phase and three degree of freedom in the transfer phase. Therefore, the angles φ_1 and φ_2 and the distance *S*, which define the positions of the leg elements, can not be calculated only in term of the coordinates X_A, Y_A. In other words, an unknown must.

be specified irrespective of the coordinates of the center of the pair *A*. In consequence, the foot (**3**) always may step on the land with the flat surface of the sole. The robot body may be moved with respect to the terrain without the changing of foot (**3**) position. This walking

possibility is not similarly with human walking and may be achieved only if the velocity and acceleration of the robot body is small. In general, the foot can be support on the land both with the flat surface and the curved front and rear ends. The plane surface of the sole and the cylindrical surface of the front end are tangent along of the generatrix *R* with respect to the mobile coordinate axes system is given by the coordinates x_{3R} and y_{3R}. The size of the flat surface of the foot, i.e. the position of the generatrix *R*, is determined from statically stability conditions in the rest state of the robot. The directrix curve of the cylindrical surface of the front end is defined by the parametrical equations

$$x_3 = x_3(\lambda),\ y_3 = y_3(\lambda)$$

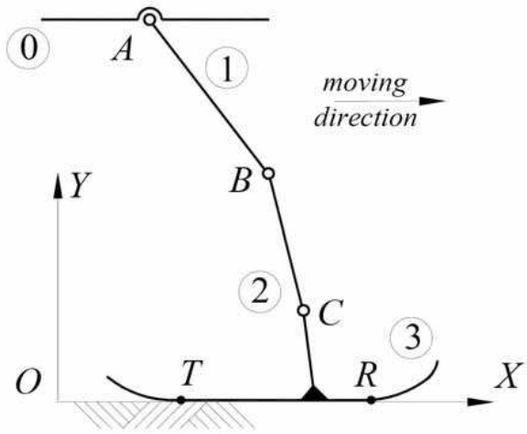

Fig. 17. Kinematics scheme of the an anthropomorphous leg

with respect to the mobile coordinate axes system attached to this element.
The generatrix in which the plane surface of the foot is tangent with the cylindrical surface of the front end is positioned by the parameter λ_0:

$$x_{3R} = x_3(\lambda_0),\ y_{3R} = y_3(\lambda_0).$$

8.1. Kinematics Analysis of the Leg Mechanism

In the support phase, when the flat surface of the foot is in contact with the terrain (Fig. 18.*a*), the analysis equations are:

$$\begin{aligned} X_A + AB\cos\varphi_1 + BC\cos\varphi_2 - S = 0; \\ Y_A + AB\sin\varphi_1 + BC\sin\varphi_2 - x_{3R} = 0. \end{aligned} \quad (24)$$

The system is indeterminate because contains three unknowns, namely φ_1, φ_2 and *S*. In order to solve it, the value of an unknown must be imposed, for example the angle φ_1. It is considered as known the position of the pair axis *A*. In this hypothesis, the solutions of the system (24) are:

$$\varphi_2 = \arccos \frac{\sqrt{BC^2 - (x_{3R} - Y_A - AB\sin\varphi_1)^2}}{BC}$$

$$\text{or } \varphi_2 = \arcsin\frac{x_{3R} - Y_A - AB\sin\varphi_1}{BC};$$

$$S = \sqrt{BC^2 - (x_{3R} - Y_A - AB\sin\varphi_1)^2}\ .$$

The coordinates of the tangent point R have the expressions:

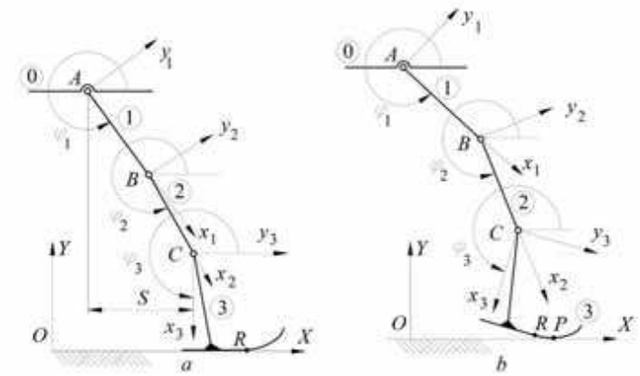

Fig. 18. The leg in the support phase

$$X_R = X_A + \sqrt{BC^2 - (x_{3R} - Y_A - AB\sin\varphi_1)^2} + y_{3R}$$
$$Y_R = 0\,.$$

In the end of the support phase, when the contact of the foot with the land is made along the generatrix which passes through the P point (Fig. 18.*b*), the analysis equations are:

$$\begin{aligned} &Y_A + AB\sin\varphi_1 + BC\sin\varphi_2 + CP\sin(\varphi_3 + u) = Y_P;\\ &X_A + AB\cos\varphi_1 + BC\cos\varphi_2 + CP\cos(\varphi_3 + u) = X_P;\\ &\frac{\left.\frac{dx_3}{d\lambda}\right|_{\lambda=\lambda_P}}{\left.\frac{dy_3}{d\lambda}\right|_{\lambda=\lambda_P}} = -\tan\varphi_3\,, \end{aligned} \tag{25}$$

where: $u = \arctan\dfrac{y_3(\lambda_P)}{x_3(\lambda_P)}$; $CP = \sqrt{x_3^2(\lambda_P) + y_3^2(\lambda_P)}$;

λ_P is the value of the λ parameter which corresponds to the generatrix which passes through the P point of the directrix curve;

$$X_P = X_R + \int_{\lambda_0}^{\lambda_P}\sqrt{\left(\frac{dx_3}{d\lambda}\right)^2 + \left(\frac{dy_3}{d\lambda}\right)^2}\,d\lambda\,,$$

because it is assumed that the foot sole do not slipped on the land surface.

The equations (25) are solved with respect to the unknowns φ_2, φ_3 and λ_P. in term of the coordinates X_A, Y_A and the angle φ_1.

By differentiation with respect to the time of the equations (25), result the velocity transmission functions:

$$\frac{\mathrm{d}Y_A}{\mathrm{d}t} + AB\cos\varphi_1\frac{\mathrm{d}\varphi_1}{\mathrm{d}t} + BC\cos\varphi_2\frac{\mathrm{d}\varphi_2}{\mathrm{d}t} + CP\cos(\varphi_3+u)\left(\frac{\mathrm{d}\varphi_3}{\mathrm{d}t} + \frac{\mathrm{d}u}{\mathrm{d}\lambda}\frac{\mathrm{d}\lambda}{\mathrm{d}t}\right) + \frac{\mathrm{d}CP}{\mathrm{d}\lambda}\sin(\varphi_3+u)\frac{\mathrm{d}\lambda}{\mathrm{d}t} = 0;$$

$$AB\sin\varphi_1\frac{\mathrm{d}\varphi_1}{\mathrm{d}t} + BC\sin\varphi_2\frac{\mathrm{d}\varphi_2}{\mathrm{d}t} + CP\sin(\varphi_3+u)\left(\frac{\mathrm{d}\varphi_3}{\mathrm{d}t} + \frac{\mathrm{d}u}{\mathrm{d}\lambda}\frac{\mathrm{d}\lambda}{\mathrm{d}t}\right) - \frac{\mathrm{d}CP}{\mathrm{d}\lambda}\cos(\varphi_3+u)\frac{\mathrm{d}\lambda}{\mathrm{d}t} + \frac{\mathrm{d}X_P}{\mathrm{d}\lambda}\frac{\mathrm{d}\lambda}{\mathrm{d}t} - \frac{\mathrm{d}X_A}{\mathrm{d}t} = 0; \quad (26)$$

$$\frac{\dfrac{\mathrm{d}^2y_3}{\mathrm{d}\lambda^2}\dfrac{\mathrm{d}x_3}{\mathrm{d}\lambda} - \dfrac{\mathrm{d}^2x_3}{\mathrm{d}\lambda^2}\dfrac{\mathrm{d}y_3}{\mathrm{d}\lambda}}{\left(\dfrac{\mathrm{d}y_3}{\mathrm{d}\lambda}\right)^2}\frac{\mathrm{d}\lambda}{\mathrm{d}t} - \frac{1}{\cos^2\varphi_3}\frac{\mathrm{d}\varphi_3}{\mathrm{d}t} = 0,$$

which are simultaneous solved with respect to the unknowns $\frac{\mathrm{d}\varphi_2}{\mathrm{d}t}$, $\frac{\mathrm{d}\varphi_3}{\mathrm{d}t}$ and $\frac{\mathrm{d}\lambda}{\mathrm{d}t}$,

where: $$\frac{\mathrm{d}u}{\mathrm{d}t} = \frac{\dfrac{\mathrm{d}y_3}{\mathrm{d}\lambda}x_3(\lambda) - \dfrac{\mathrm{d}x_3}{\mathrm{d}\lambda}y_3(\lambda)}{x_3^2(\lambda) + y_3^2(\lambda)}\frac{\mathrm{d}\lambda}{\mathrm{d}t},$$

$$\frac{\mathrm{d}CP}{\mathrm{d}t} = \frac{x_2(\lambda)\dfrac{\mathrm{d}x_2}{\mathrm{d}\lambda} + y_2(\lambda)\dfrac{\mathrm{d}y_2}{\mathrm{d}\lambda}}{CP}\frac{\mathrm{d}\lambda}{\mathrm{d}t},$$

$$\frac{\mathrm{d}X_P}{\mathrm{d}t} = \frac{\mathrm{d}}{\mathrm{d}\lambda}\left[\int_{\lambda_0}^{\lambda}\sqrt{\left(\frac{\mathrm{d}x_3}{\mathrm{d}\lambda}\right)^2 + \left(\frac{\mathrm{d}y_3}{\mathrm{d}\lambda}\right)^2}\,\mathrm{d}\lambda\right]\frac{\mathrm{d}\lambda}{\mathrm{d}t}.$$

Further on, by differentiation the equations (26) result the acceleration transmission functions:

$$\frac{\mathrm{d}^2Y_A}{\mathrm{d}t^2} + AB\left[\cos\varphi_1\frac{\mathrm{d}^2\varphi_1}{\mathrm{d}t^2} - \sin\varphi_1\left(\frac{\mathrm{d}\varphi_1}{\mathrm{d}t}\right)^2\right] + BC\left[\cos\varphi_2\frac{\mathrm{d}^2\varphi_2}{\mathrm{d}t^2} - \sin\varphi_2\left(\frac{\mathrm{d}\varphi_2}{\mathrm{d}t}\right)^2\right] +$$

$$+ CP\cos(\varphi_3+u)\left(\frac{\mathrm{d}^2\varphi_3}{\mathrm{d}t^2} + \frac{\mathrm{d}^2u}{\mathrm{d}\lambda^2}\left(\frac{\mathrm{d}\lambda}{\mathrm{d}t}\right)^2 + \frac{\mathrm{d}u}{\mathrm{d}\lambda}\frac{\mathrm{d}^2\lambda}{\mathrm{d}t^2}\right) - CP\sin(\varphi_3+u)\left(\frac{\mathrm{d}\varphi_3}{\mathrm{d}t} + \frac{\mathrm{d}u}{\mathrm{d}\lambda}\frac{\mathrm{d}\lambda}{\mathrm{d}t}\right)^2 +$$

$$+ \frac{\mathrm{d}^2CP}{\mathrm{d}\lambda^2}\sin(\varphi_3+u)\left(\frac{\mathrm{d}\lambda}{\mathrm{d}t}\right)^2 + 2\frac{\mathrm{d}CP}{\mathrm{d}\lambda}\cos(\varphi_3+u)$$

$$\left(\frac{\mathrm{d}\varphi_3}{\mathrm{d}t}+\frac{\mathrm{d}u}{\mathrm{d}\lambda}\frac{\mathrm{d}\lambda}{\mathrm{d}t}\right)\frac{\mathrm{d}\lambda}{\mathrm{d}t}+\frac{\mathrm{d}CP}{\mathrm{d}\lambda}\sin(\varphi_3+u)\frac{\mathrm{d}^2\lambda}{\mathrm{d}t^2}=0;$$

$$AB\left[\sin\varphi_1\frac{\mathrm{d}^2\varphi_1}{\mathrm{d}t^2}+\cos\varphi_1\left(\frac{\mathrm{d}\varphi_1}{\mathrm{d}t}\right)^2\right]+BC\left[\sin\varphi_2\frac{\mathrm{d}^2\varphi_2}{\mathrm{d}t^2}+\cos\varphi_2\left(\frac{\mathrm{d}\varphi_2}{\mathrm{d}t}\right)^2\right]+$$

$$+CP\sin(\varphi_3+u)\left(\frac{\mathrm{d}^2\varphi_3}{\mathrm{d}t^2}+\frac{\mathrm{d}^2u}{\mathrm{d}\lambda^2}\left(\frac{\mathrm{d}\lambda}{\mathrm{d}t}\right)^2+\frac{\mathrm{d}u}{\mathrm{d}\lambda}\frac{\mathrm{d}^2\lambda}{\mathrm{d}t^2}\right)+$$

$$+\ CP\cos(\varphi_3+u)\left(\frac{\mathrm{d}\varphi_3}{\mathrm{d}t}+\frac{\mathrm{d}u}{\mathrm{d}\lambda}\frac{\mathrm{d}\lambda}{\mathrm{d}t}\right)^2+\frac{\mathrm{d}^2X_P}{\mathrm{d}\lambda^2}\left(\frac{\mathrm{d}\lambda}{\mathrm{d}t}\right)^2+$$

$$+2\frac{\mathrm{d}CP}{\mathrm{d}\lambda}\sin(\varphi_3+u)\left(\frac{\mathrm{d}\varphi_3}{\mathrm{d}t}+\frac{\mathrm{d}u}{\mathrm{d}\lambda}\frac{\mathrm{d}\lambda}{\mathrm{d}t}\right)\frac{\mathrm{d}\lambda}{\mathrm{d}t}-\frac{\mathrm{d}^2X_A}{\mathrm{d}t^2}-\frac{\mathrm{d}^2CP}{\mathrm{d}\lambda^2}\cos(\varphi_3+u)\left(\frac{\mathrm{d}\lambda}{\mathrm{d}t}\right)^2-\frac{\mathrm{d}CP}{\mathrm{d}\lambda}\cos$$

$$(\varphi_3+u)\frac{\mathrm{d}^2\lambda}{\mathrm{d}t^2}=0;$$

$$\frac{\left(\frac{\mathrm{d}^3y_3}{\mathrm{d}\lambda^3}\frac{\mathrm{d}x_3}{\mathrm{d}\lambda}-\frac{\mathrm{d}^3x_3}{\mathrm{d}\lambda^3}\frac{\mathrm{d}y_3}{\mathrm{d}\lambda}\right)\frac{\mathrm{d}x_3}{\mathrm{d}\lambda}-2A\frac{\mathrm{d}^2x_3}{\mathrm{d}\lambda^2}}{\left(\frac{\mathrm{d}y_3}{\mathrm{d}\lambda}\right)^3}\left(\frac{\mathrm{d}\lambda}{\mathrm{d}t}\right)^2+$$

$$\frac{A}{\left(\frac{\mathrm{d}x_3}{\mathrm{d}\lambda}\right)^2}\frac{\mathrm{d}^2\lambda}{\mathrm{d}t^2}-\frac{2\sin\varphi_3}{\cos\varphi_3^3}\left(\frac{\mathrm{d}\varphi_3}{\mathrm{d}t}\right)^2-\frac{1}{\cos^2\varphi_3}\frac{\mathrm{d}^2\varphi_3}{\mathrm{d}t^2}=0,$$

$$\text{where } A=\frac{\mathrm{d}^2y_3}{\mathrm{d}\lambda^2}\frac{\mathrm{d}x_3}{\mathrm{d}\lambda}-\frac{\mathrm{d}^2x_3}{\mathrm{d}\lambda^2}\frac{\mathrm{d}y_3}{\mathrm{d}\lambda},$$

which are simultaneous solved with respect to the unknowns $\frac{\mathrm{d}^2\varphi_2}{\mathrm{d}t^2}$, $\frac{\mathrm{d}^2\varphi_3}{\mathrm{d}t^2}$ and $\frac{\mathrm{d}^2\lambda}{\mathrm{d}t^2}$

where:

$$\frac{\mathrm{d}^2u}{\mathrm{d}t^2}=\left[\frac{\frac{\mathrm{d}^2y_3}{\mathrm{d}\lambda^2}x_3(\lambda)-\frac{\mathrm{d}^2x_3}{\mathrm{d}\lambda^2}y_3(\lambda)}{x_3^2(\lambda)+y_3^2(\lambda)}-\right.$$

$$\left.-2\frac{\frac{\mathrm{d}x_3}{\mathrm{d}\lambda}\frac{\mathrm{d}y_3}{\mathrm{d}\lambda}\left(x_3^2(\lambda)-y_3^2(\lambda)\right)-x_3(\lambda)y_3(\lambda)Q}{\left(x_3^2(\lambda)+y_3^2(\lambda)\right)^2}\right]\left(\frac{\mathrm{d}\lambda}{\mathrm{d}t}\right)^2+$$

$$+\frac{\frac{\mathrm{d}y_3}{\mathrm{d}\lambda}x_3(\lambda)-\frac{\mathrm{d}x_3}{\mathrm{d}\lambda}y_3(\lambda)}{x_3^2(\lambda)+y_3^2(\lambda)}\frac{\mathrm{d}^2\lambda}{\mathrm{d}t^2};$$

$$Q = \left(\frac{\mathrm{d}x_3}{\mathrm{d}\lambda}\right)^2 - \left(\frac{\mathrm{d}y_3}{\mathrm{d}\lambda}\right)^2 .$$

8.2. Forces Distribution in the Leg Mechanism

The goal of the forces analysis in the leg mechanism is the determination of the conditions of the static stability of the feet and of the whole robot. The leg mechanism is plane, and the reaction forces from the pairs are within the motion plane. The pressure on the contact surface or generatrix is assumed to be equally distributed. From the equilibrium equations of the forces which act on the leg mechanism elements (Fig. 19), the reaction forces from pairs *A*, *B* and *C* and the modulus and the origin of the normal reaction *N* are calculated. If the position of the origin of normal reaction force *N* results outside of the support surface, the foot overturns and walking robot lose its static stability. To avoid this phenomenon it is enforce that the origin of the normal reaction force to fill a certain position, definite by the distance *d*. In this case, a driving moment in the pair *A*, applied between the body (**0**) and the thigh (**1**) is added. This moment is the sixth unknown quantity of the forces distribution problem.

Taking into consideration the particularities of the contact between terrain and foot, the leg mechanism is analyzed in the following way:

- first: it is solved the equations (27), which define the equilibrium of the forces acting on the elements (**1**) and (**2**),
- second: it is solved the equations (28), which express the equilibrium of the forces acting on the foot (**3**).

The particularities consist in the fact that the foot (**3**) is supported or rolled without sliding on terrain.

As a result, the reaction force acting to the foot (**3**) has two components, namely $\overline{N}$ along the normal on the support plane and $\overline{T}$ holds in the support plane. The rolled without the front or rear end of the foot slide if $T < \mu N$ only, where μ is the frictional coefficient between foot and terrain.

The forces analysis is made in two situations.

1. The foot is supported with his flat surface on the terrain (Fig. 19.*a*).

The equations of the forces analysis which act on the links (**1**) and (**2**) are:

$$\begin{gathered}
Q_X + F_{i1X} - R_{12X} + R_{01X} = 0; \\
Q_Y + F_{i1Y} - m_1 g - R_{12Y} + R_{01Y} = 0; \\
M_{01} + (F_{i1Y} - m_1 g)(X_{G1} - X_B) - F_{i1X}(Y_{G1} - Y_B) + R_{01X}(Y_A - Y_B) + R_{01Y}(X_B - X_A) + M_{i1} = 0; \\
F_{i2X} + R_{12X} + R_{32X} = 0; \\
F_{i2Y} - m_2 g + R_{12Y} + R_{32Y} = 0; \\
(F_{i2Y} - m_2 g)(X_{G2} - X_B) - F_{12X}(Y_{G2} - Y_B) + R_{32Y}(X_C - X_B) - R_{32X}(Y_C - Y_B) + M_{i2} = 0,
\end{gathered} \tag{27}$$

where $M_{01} = 0$.

$\overline{Q} = Q_x \bar{i} + Q_y \bar{j}$ is the direct acting load on the leg in the center of the pair *A*;

$$F_{ijX} = -m_j \frac{\mathrm{d}^2 X_{Gj}}{\mathrm{d}t^2}, \; F_{ijY} = -m_j \frac{\mathrm{d}^2 Y_{Gj}}{\mathrm{d}t^2},$$

$$M_{ij} = -I_{Gj}\frac{\mathrm{d}^2\varphi_j}{\mathrm{d}t^2};\ j=\overline{1,3},$$

$$\frac{\mathrm{d}^2X_{G1}}{\mathrm{d}t^2} = \frac{\mathrm{d}^2X_A}{\mathrm{d}t^2} - (x_{1G1}\sin\varphi_1 + y_{1G1}\cos\varphi_1)\frac{\mathrm{d}^2\varphi_1}{\mathrm{d}t^2} -$$
$$-(x_{1G1}\cos\varphi_1 - y_{1G1}\sin\varphi_1)\left(\frac{\mathrm{d}\varphi_1}{\mathrm{d}t}\right)^2;$$

$$\frac{\mathrm{d}^2Y_{G1}}{\mathrm{d}t^2} = \frac{\mathrm{d}^2Y_A}{\mathrm{d}t^2} + (x_{1G1}\cos\varphi_1 - y_{1G1}\sin\varphi_1)\frac{\mathrm{d}^2\varphi_1}{\mathrm{d}t^2} -$$
$$-(x_{1G1}\sin\varphi_1 + y_{1G1}\cos\varphi_1)\left(\frac{\mathrm{d}\varphi_1}{\mathrm{d}t}\right)^2;$$

$$\frac{\mathrm{d}^2X_{G2}}{\mathrm{d}t^2} = \frac{\mathrm{d}^2X_A}{\mathrm{d}t^2} - (x_{2G2}\sin\varphi_2 + y_{2G2}\cos\varphi_2)\frac{\mathrm{d}^2\varphi_2}{\mathrm{d}t^2} -$$
$$-(x_{2G2}\cos\varphi_2 - y_{2G2}\sin\varphi_2)\left(\frac{\mathrm{d}\varphi_2}{\mathrm{d}t}\right)^2 -$$
$$-AB(\sin\varphi_1\frac{\mathrm{d}^2\varphi_1}{\mathrm{d}t^2} + \cos\varphi_1\left(\frac{\mathrm{d}\varphi_1}{\mathrm{d}t}\right)^2);$$

$$\frac{\mathrm{d}^2Y_{G2}}{\mathrm{d}t^2} = \frac{\mathrm{d}^2Y_A}{\mathrm{d}t^2} + (x_{2G2}\cos\varphi_2 - y_{2G2}\sin\varphi_2)\frac{\mathrm{d}^2\varphi_2}{\mathrm{d}t^2} -$$
$$-(x_{2G2}\sin\varphi_2 + y_{2G2}\cos\varphi_2)\left(\frac{\mathrm{d}\varphi_2}{\mathrm{d}t}\right)^2 -$$
$$+AB(\cos\varphi_1\frac{\mathrm{d}^2\varphi_1}{\mathrm{d}t^2} - \sin\varphi_1\left(\frac{\mathrm{d}\varphi_1}{\mathrm{d}t}\right)^2);$$

$$\frac{\mathrm{d}^2X_{G3}}{\mathrm{d}t^2} = \frac{\mathrm{d}^2X_A}{\mathrm{d}t^2} - (x_{3G3}\sin\varphi_3 + y_{3G3}\cos\varphi_3)\frac{\mathrm{d}^2\varphi_3}{\mathrm{d}t^2} -$$
$$-(x_{3G3}\cos\varphi_3 - y_{3G3}\sin\varphi_3)\left(\frac{\mathrm{d}\varphi_3}{\mathrm{d}t}\right)^2 - AB(\sin\varphi_1\frac{\mathrm{d}^2\varphi_1}{\mathrm{d}t^2} +$$
$$+\cos\varphi_1\left(\frac{\mathrm{d}\varphi_1}{\mathrm{d}t}\right)^2) - BC(\sin\varphi_2\frac{\mathrm{d}^2\varphi_2}{\mathrm{d}t^2} + \cos\varphi_2\left(\frac{\mathrm{d}\varphi_2}{\mathrm{d}t}\right)^2);$$

$$\frac{\mathrm{d}^2Y_{G3}}{\mathrm{d}t^2} = \frac{\mathrm{d}^2Y_A}{\mathrm{d}t^2} + (x_{3G3}\cos\varphi_3 - y_{3G3}\sin\varphi_3)\frac{\mathrm{d}^2\varphi_3}{\mathrm{d}t^2} -$$
$$-(x_{3G3}\sin\varphi_3 + y_{3G3}\cos\varphi_3)\left(\frac{\mathrm{d}\varphi_3}{\mathrm{d}t}\right)^2 + AB(\cos\varphi_1\frac{\mathrm{d}^2\varphi_1}{\mathrm{d}t^2} -$$
$$-\sin\varphi_1\left(\frac{\mathrm{d}\varphi_1}{\mathrm{d}t}\right)^2) + BC(\cos\varphi_2\frac{\mathrm{d}^2\varphi_2}{\mathrm{d}t^2} - \sin\varphi_2\left(\frac{\mathrm{d}\varphi_2}{\mathrm{d}t}\right)^2).$$

The equations (4) are simultaneous solved with respect to the unknowns R_{01X}, R_{01Y}, R_{12X}, R_{12Y}, R_{32X} and R_{32Y}.

The reaction force $\overline{R}_{ij} = R_{ijX}\bar{i} + R_{ijY}\bar{j}$ acts from the link (*i*) to the link (*j*).

Equations which expressing the equilibrium of the forces which act on the foot (**3**) are:

$$\begin{gathered} T - R_{32X} = 0; \\ N - R_{32Y} - m_3 g = 0; \\ N d + T Y_C - m_3 g (X_{G3} - X_C) = 0, \end{gathered} \tag{28}$$

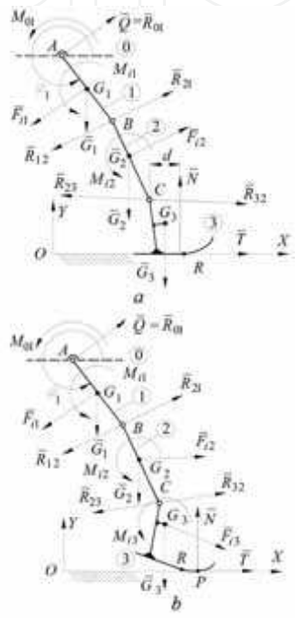

Fig. 19. Forces distribution in the leg mechanism

These equations are solved with respect to the unknowns *N*, *T* and *d*. If $T > \mu N$, the foot slipped on the terrain. In this case, the input moment $M_{01} \neq 0$ must be applied to the thigh (**1**). The magnitude of this moment is calculated by solving of the equations (27), where $R_{32X} < \mu N$. The sets of equations (27) and (28) are solved iteratively, until the difference between two successive iterations decreases under a certain limit.

2. The foot is supported with his front end on the terrain (Fig. 19.*b*)

The foot (**3**) may be in this position if a driving moment is applied in pair *C*, between links (**2**) and (**3**). The reaction forces from pair *A* and *B* are the solutions of the equations (29):

$$\begin{gathered} Q_X + F_{i1X} - R_{12X} + R_{01X} = 0; \\ Q_Y + F_{i1Y} - m_1 g - R_{12Y} + R_{01Y} = 0; \\ M_{01} + (F_{i1Y} - m_1 g)(X_{G1} - X_B) - F_{i1X} (Y_{G1} - Y_B) + R_{01X}(Y_A - Y_B) + R_{01Y}(X_B - X_A) + M_{i1} = 0; \\ F_{i2X} + R_{12X} + R_{32X} = 0; \\ F_{i2Y} - m_2 g + R_{12Y} + R_{32Y} = 0; \\ (F_{i2Y} - m_2 g)(X_{G2} - X_B) - F_{12X} (Y_{G2} - Y_B) + R_{32Y}(X_C - X_B) - R_{32X} (Y_C - Y_B) + M_{i2} - M_{23} = 0, \end{gathered} \tag{29}$$

where $M_{01} = M_{23} = 0$.
The unknowns of these equations are R_{01X}, R_{01Y}, R_{12X}, R_{12Y}, R_{32X} and R_{32Y}.
Equilibrium of the forces which act on the foot (**3**) is expressed by equations (30):

$$T - R_{32X} + F_{i3X} = 0;$$
$$N - R_{32Y} - m_3 g + F_{i3Y} = 0; \quad (30)$$
$$M_{23} + M_{i3} + N (X_P - X_C) + T Y_C + (F_{i3Y} - m_3 g) (X_{G3} - X_C) - F_{i3X}(Y_{G3} - Y_C) = 0.$$

Solutions of these equations are N, T and M_{23}. If $T > \mu N$, the foot slipped on the terrain and the robot overturns.

8.3. Optimum Design of the Foot

The bottom surface of the foot of a walking robot may have various shapes. These surfaces differ by the size of the flat surface and the forms of the front and rear cylindrical surfaces. The most adequate form of the bottom surface of the foot, i.e. the expressions of the directrices of the front and rear cylindrical surfaces, is determined by optimization of some parameters. The objective function (Fox R. 1973), (Goldberg D. 1999), (Coley D. 1999), which is minimized in the optimization process may expressed:

- maximum angular velocity or $\frac{d^2\varphi_3}{d^2t}$;
- the maximum driving forces or moments;
- etc.

The unknowns which respect to the objective function is minimized are:

- the lengths AB and BC of the links (**1**) and (**2**),
- the coordinate x_{3R}, y_{3R} of the point R;
- the coefficients from the equations of the directrices curves of the surfaces of the front and rear ends.

The minimization of the objective function is performed in the presence of constrains which expressed:

- the directrix curves of the front and rear ends are tangent to the flat surface of the foot sole,
- the ordinate y_{3R} and y_{3T} of the points R and T respectively in which the directrix curves are tangent to the flat surfaces are limit by the minimum flat surface of the foot, to provide the static stability of the robot which rest.

9. Conclusions

The walking robots are used to unconventional displacement of the technological loads over the unarranged terrains. The modular constructions of the walking robots led to a more suppleness and very good adaptation to any terrain surface. The displacement is carried out at the very most circumstances and with a minimum expenditure of energy if the leg mechanisms are designed in accordance with the above prescriptions

10. References

Appel P., (1908). *Trataité de Mécanique Rationnelle*, Gauthier-Villars, Paris

Bares J. E., European Patent no A1 0399720.

Bessonov A.P., Umnov N.V. (1973). *The Analysis of gaits in six legeed Vehicles according to their static stability* Proc. Theory and Practice of Robots and Manipulators, Udine, Italy

Buzdugan Gh., (1980) *Material Strength*, Ed. Didactică şi Pedagogică, Bucarest, (in Romanian)

Coley D. (1999). *An Introduction to Genetic Algorithms for Scientists and Engineers*, World Scientific

Denavit J., Hartenberg R.S. (1955). .*A kinematic notation for lower-pair mechanisms based on matrices*, Journal of Applied Mechanics, no.22

Ebert-Uphoff I., Gosselin C.,M. (1998). *Static Balancing of a Class of Spatial Parallel Platform Mechanisms,* Proceeding of the ASME Mechanisms Conference, Atlanta, USA

Fox R. (1973). *Optimization Methods for Engineering Design*, Addison Wesley Publishing Comp,

Garrec P., *U. S. Patent* no 5219410

Goldberg D. (1999). *Genetic Algorithms in Search, Optimisation and Machine Learning*, Addison Wesley Publishing Comp.

Hildegrand F.B. (1956). *Introduction in Numerical Analysis*, McGraw Hill Book Company

Hiller M., Muller J., Roll U., Schneider M., Scroter D., Torlo M., Ward D. (1999). .*Design and Realization of the Anthropomorphically Legged and Wheeled Duisburg Robot Alduro*, The Tenth World Congress on the Theory of Machines and Mechanisms, Oulu, Finland, June 20-24

Hirose S. (1991). *Three Basic Types of Locomotion in Mobile Robots*, IEEE, pp. 12-17

Ion I., Stefanescu D.M. (1999). .*Force Distribution in the MERO Four-Legged Walking Robot"*, ISMCR'99 - Topical Workshop on Virtual Reality and Advanced Human-Robot Systems, vol X, Tokyo, Japan, June 10-11

Ion I., Simionescu I., Ungureanu M. (2001). *Discreet static balancing of the walking robots shifting systems mechanisms*, The Annual Symposium of the Institute of Solid Mechanisms – SISOM' 2001, Bucharest, May 24-25, , pp 202-207

Ion I., Simionescu I., Curaj A. (2002). *MERO modular walking robot having applications in farming and forestry* The 5thInternational Conference on Climbing and Walking Robots, September 25-27, -Paris –France

Ion I., Ungureanu M., Simionescu I. (2000). *Control System of MERO modular Walking Robot,* Proceedings of the International Conference on Manufacturing Systems, Bucharest, October 10-11, Romanien Academy Publishing House, pp 351-354 ISBN 973-27-0932-4.

Ion I., Simionescu I., Curaj A. (2002). *Mobil Mechatronic System With Applications in Agriculture and Sylviculture*. The 2thIFAC International Conference on Mechatronic Systems, December 8-12, -Berkeley University – USA

Ion I., Simionescu I., Curaj A. (2003). *The displasement of Quatrupedal Walking Robots,* Proceedings of the 11th World Congress in Mechanism and Machine Science, August 18-21, Tianjin – China.

Ion I**.,** Simionescu I., Curaj A.*,* Ungureanu M (2004). *MERO modular Walking robot support of technological equipments* International Conference of Robots, Timisoara, 0ct. 14 -17, Romania

Kumar V., Waldron K.J. (1988). *Force Distribution in Closed Kinematics Chain,*: IEEE Journal of Robotic and Automation, Vol. 4, No. 6, pp. 657-664.

Kumar V., Waldron K.J. (1988). *Force Distribution in Walking Vehicle*, Proc. 20th ASME Mechanism Conference, Orlando, Florida, Vol. DE-3, pp. 473-480.

McGhee R.B., Frank A.A. (1968). *Stability Properties of Quadruped Creeping Gait*, *Mathematical Biosciences*, Vol. 3, No.2, pp. 331-351

McGhee, R.B., Orin, D.E. (1976). *A* M*athematical Programming Approach to Control of Joint Positions and Torques in Legged Locomotion Systems,*: Proc. 2nd CISM -IFToMM Conference for the Theory and Practice of Robot Manipulators (ROMANSY), Warsaw, Poland, Sept. 14-17, pp. 225-231

Nishikawa Masao et al. (1999). European Patent no. 0433091A2

Okhotsimski D.E., Golubev I., (1984). *Mehanica i upravleniae dvijeniem avtomaticeskovo sgaiuscevo aparata*, Moscwa, "Nauka"

Rossman T., Pfeiffer F(1999). *Control of tube Crawling Robot*, Automatisierungstechnik 47, Oldenbourg Verlag.

Simionescu I., Moise V. (1999), *Mechanisms*, Technical Publishing House, Bucarest,. (in romanian)

Simionescu I., Ion I., Ciupitu L. (1996). *Optimization of Walking Robots Movement Systems*, Proceedings of the VII International Congress on the Theory of Machines and Mechanisms, Liberec, Czech Republic, 3 - 5 September,

Simionescu I., Moise V., Dranga M. (1995). *Numerical Methods in Engineering*, Technical Publishing House, Bucarest, 1995 (in romanian)

Simionescu, I, Ion.,I (2004) *Feet for two legeed Walking Robots,* 35th International Symposium on Robotics , March 23-26, Paris – France.

Simionescu I., Ion I. (2001). *Static Balancing of Walking Machines*, POLITEHNICA University of Bucharest, Sci. Bull., Series D, vol. 63 no. 1, pp.15 – 22.

Song S.M., Waldron K.J. (1989). *Machines that Walk,* Massachusetts Institute of Technology Press, 1989.

Song S.M., Lee J.K. (1988). *The Mechanical Efficiency and Kinematics Pantograph Type Manipulators*, Proceedings of the IEEE International Conference on Robotics and Automation, Philadelphia, Vol. I pp.414-420

Streit, D.,A., Gilmore, B.,J. (1989). *Perfect Spring Equilibrators for Routable Bodies*, Journal of Mechanisms, Transmissions and Automation in Design, vol. 111, pp. 451 - 458.

Uicker J.J.jr., Denavit J., Hartenberg R.S.(1965). *An Iterative Method for the Displacement Analysis of Spatial Mechanisms*, Trans. of the ASME, paper 63-WA-45.

Waldron K.J. (1985). *Force and Motion Management in Legged Locomotion,* Proceedings of the 24th IEEE Conference on Decision and Control, Fort Lauderdale, pp.12-17

Waldron K.J. (1996), *Modeling and Simulation of Human and Walking Robots Locomotion*, Advanced School, Udine, Italy,

Nishikawa Masao et al, *European Patent Application* no. 0433091A2

Climbing and Walking Robots: towards New Applications

Edited by Houxiang Zhang

ISBN 978-3-902613-16-5

Hard cover, 546 pages

Publisher I-Tech Education and Publishing

Published online 01, October, 2007

Published in print edition October, 2007

With the advancement of technology, new exciting approaches enable us to render mobile robotic systems more versatile, robust and cost-efficient. Some researchers combine climbing and walking techniques with a modular approach, a reconfigurable approach, or a swarm approach to realize novel prototypes as flexible mobile robotic platforms featuring all necessary locomotion capabilities. The purpose of this book is to provide an overview of the latest wide-range achievements in climbing and walking robotic technology to researchers, scientists, and engineers throughout the world. Different aspects including control simulation, locomotion realization, methodology, and system integration are presented from the scientific and from the technical point of view. This book consists of two main parts, one dealing with walking robots, the second with climbing robots. The content is also grouped by theoretical research and applicative realization. Every chapter offers a considerable amount of interesting and useful information.

How to reference

In order to correctly reference this scholarly work, feel free to copy and paste the following:

Ion Ion, Ion Simionescu, Adrian Curaj and Alexandru Marin (2007). Modular Walking Robots, Climbing and Walking Robots: towards New Applications, Houxiang Zhang (Ed.), ISBN: 978-3-902613-16-5, InTech, Available from: http://www.intechopen.com/books/climbing_and_walking_robots_towards_new_applications/modular_walking_robots

INTECH
open science | open minds

InTech Europe
University Campus STeP Ri
Slavka Krautzeka 83/A
51000 Rijeka, Croatia
Phone: +385 (51) 770 447
Fax: +385 (51) 686 166
www.intechopen.com

InTech China
Unit 405, Office Block, Hotel Equatorial Shanghai
No.65, Yan An Road (West), Shanghai, 200040, China
中国上海市延安西路65号上海国际贵都大饭店办公楼405单元
Phone: +86-21-62489820
Fax: +86-21-62489821

IntechOpen